Cosmology with Galaxy Clusters:
from Simulations to Euclid

Stefano Borgani
Dept. of Physics - University of Trieste
INAF – Astronomical Observatory of Trieste
IFPU – Institute for the Fundamental Physics of the Universe - Trieste

I. Galaxy Clusters as Tracers of Cosmic Evolution

II. Simulations for cluster cosmology

    II.a Calibration of the halo mass function

    II.b Biases in mass measurements

III. The present and the future of cluster cosmology (Euclid/LSST)

Talk @ GSSI, L'Aquila, 15 Jan. 2020

https://www.ifpu.it

Institute for Fundamental Physics of the Universe

The Institute for Fundamental Physics of the Universe (IFPU) is a joint initiative of the International School for Advanced Studies (SISSA), the Abdus Salam International Centre for Theoretical Physics (ICTP), the National Institute for Astrophysics (INAF) and the National Institute for Nuclear Physics (INFN). The institute aims at hosting and promoting a vigorous and innovative multi-disciplinary research program focused on investigating the fundamental laws of Nature under a Cosmological and Astrophysical perspective.

NEWS

IFPU Colloquia starting on March 21, 2019

The program of Colloquia, Seminars and Journal Clubs at the Institute for Fundamental Physics of the Universe is starting. You can find the calendar and details on IFPU scientific events at the Activities webpage.

ANNOUNCEMENTS

Call for IFPU programs now open

The Institute for Fundamental Physics of the Universe supports and hosts: Focus Week Programs, namely small-scale thematic workshops, and Team Research Programs, namely the activity of small groups developing or finalizing a project. Calls for Read more...

ANNOUNCEMENTS

Applications for long-term visits now open (first deadline: May 1, 2019)

The Institute promotes its internationalization and the development of new research lines through visits of internationally renowned scientists with leading expertise in areas within the scientific goals of the Institute. The next deadline for receiving Read more...

Part I:
Clusters as tracers of cosmic evolution

What is a galaxy cluster ?

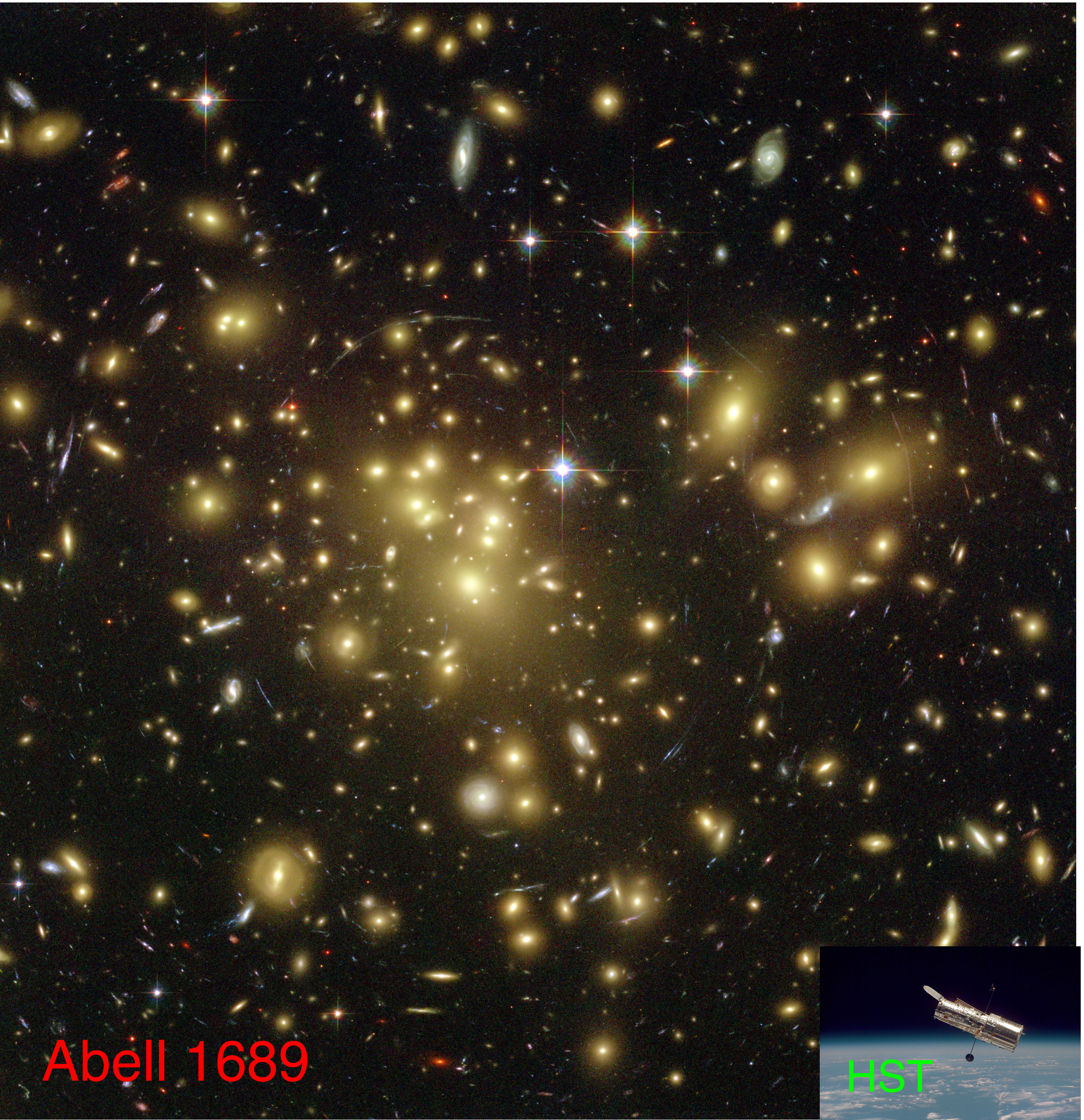

Concentrations of ~10^3 galaxies

σ_v~500-1000 km s^{-1}

Size: ~1-2 Mpc

Mass: ~10^{14}-10^{15} $M_\odot$

→ $\lambda_i \approx 10$ Mpc

What is a galaxy cluster ?

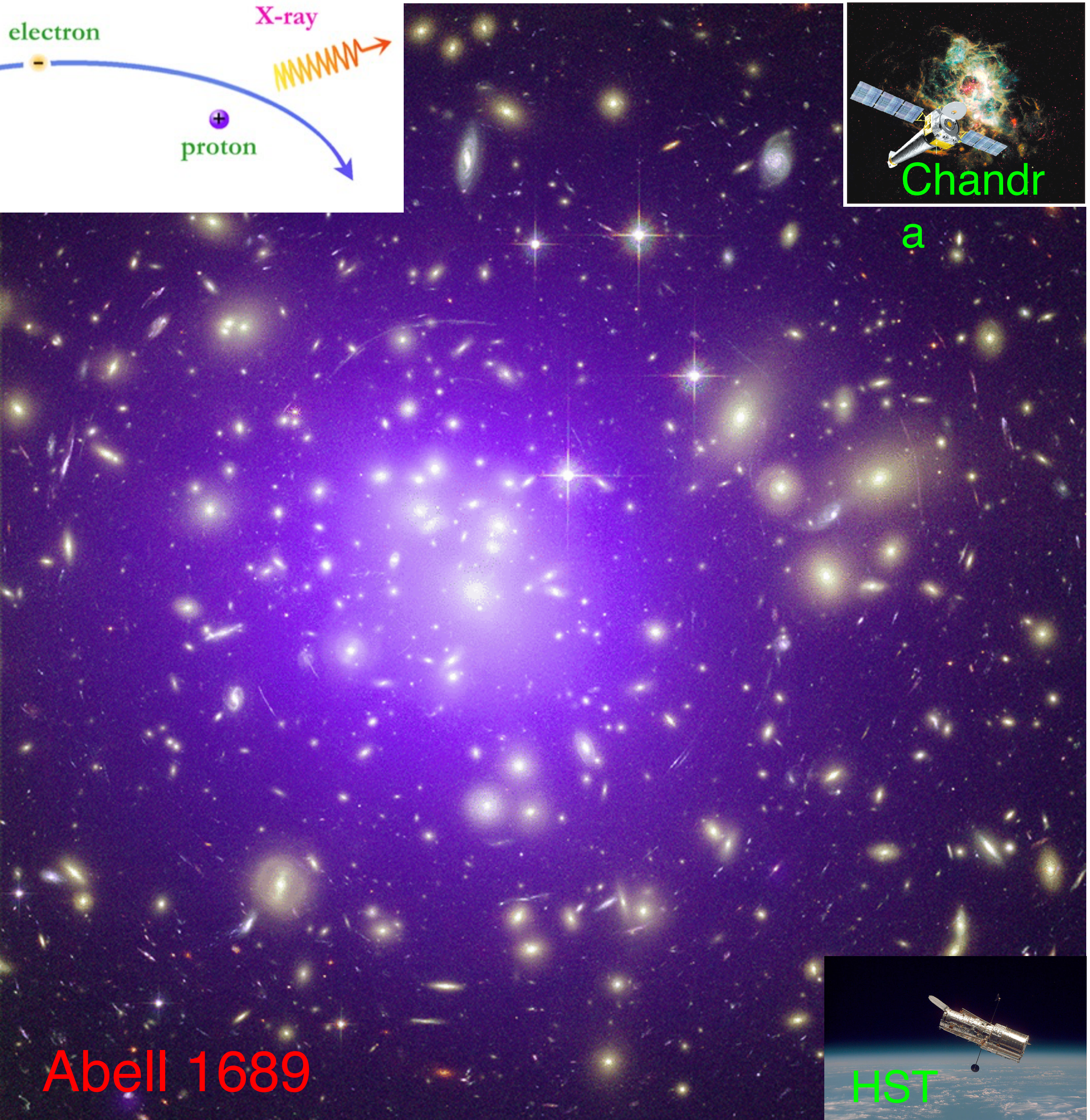

Concentrations of ~10^3 galaxies

σ_v~500-1000 km s^{-1}

Size: ~1-2 Mpc

Mass: ~10^{14}-10^{15} $M_\odot$

➔ $\lambda_i \approx 10$ Mpc

-Baryon content:

➔ cosmic share (~15%) in hydrostatic equilibrium

ICM temperature:

➔ T ~ 2-10 keV

➔ fully ionized plasma;

Thermal bremsstrahlung

➔ n_e~10^{-2}-10^{-4} cm^{-3}

➔ $L_X \sim n_e^2 V \sim 10^{45}$ erg s^{-1}

Sunyaev-Zeldovich Effect

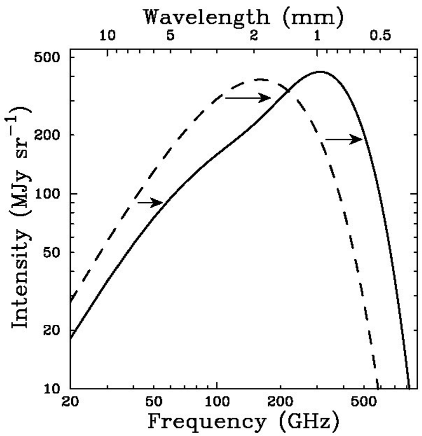

Inverse Compton scattering of CMB photons off the ICM electrons

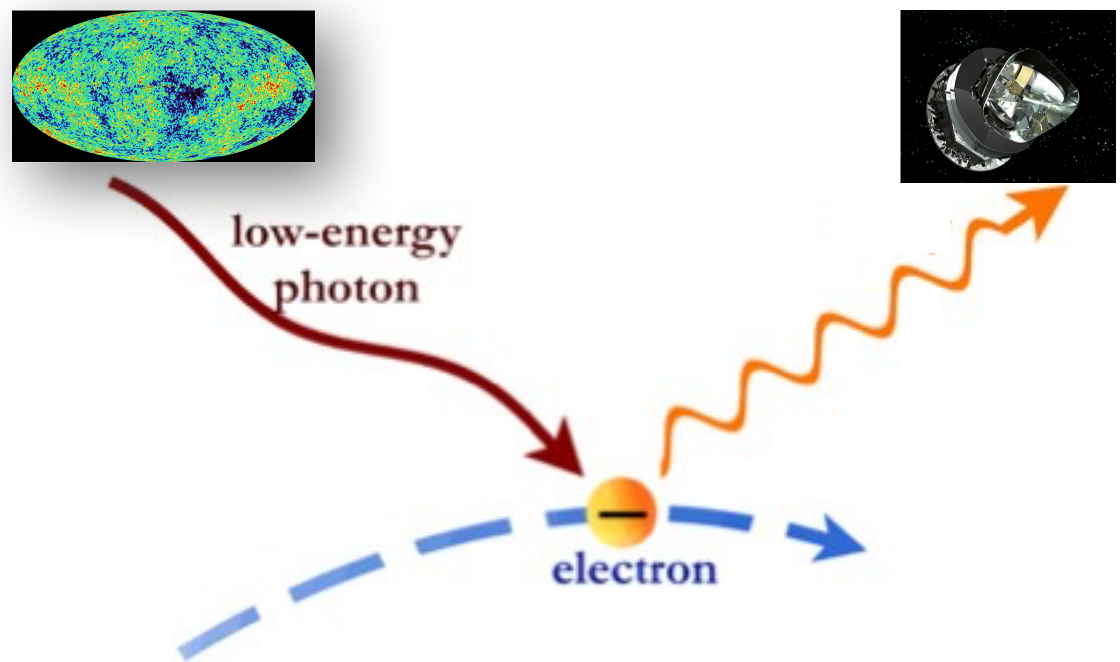

Sunyaev-Zeldovich Effect

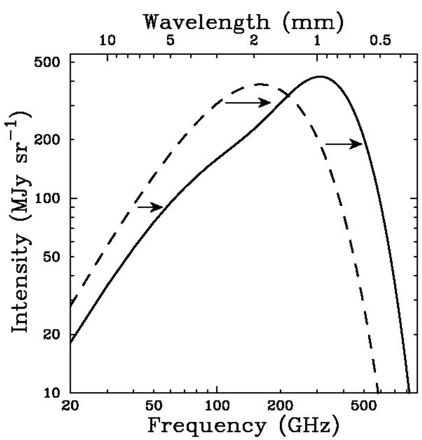

Inverse Compton scattering of CMB photons off the ICM electrons

Coma as seen by Planck

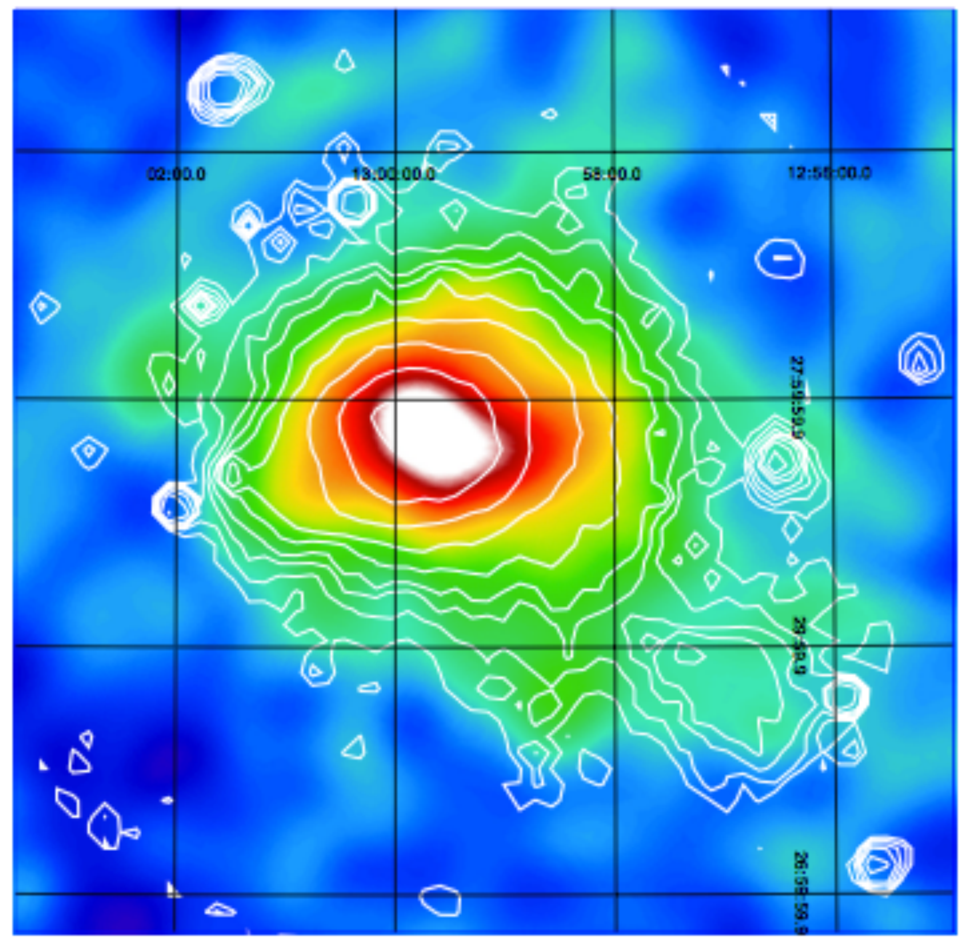

- ➔ Signal virtually independent of redshift
- ➔ Proportional to the l.o.s. integration of $n_e T_e \sim$ pressure
- ➔ Wider dynamic range accessible
- ➔ We are now in the era of SZ cluster cosmology (e.g. ACT, SPT, Planck)

Galaxy Clusters & Cosmic Growth

➔ One-to-one relationship between expansion and growth

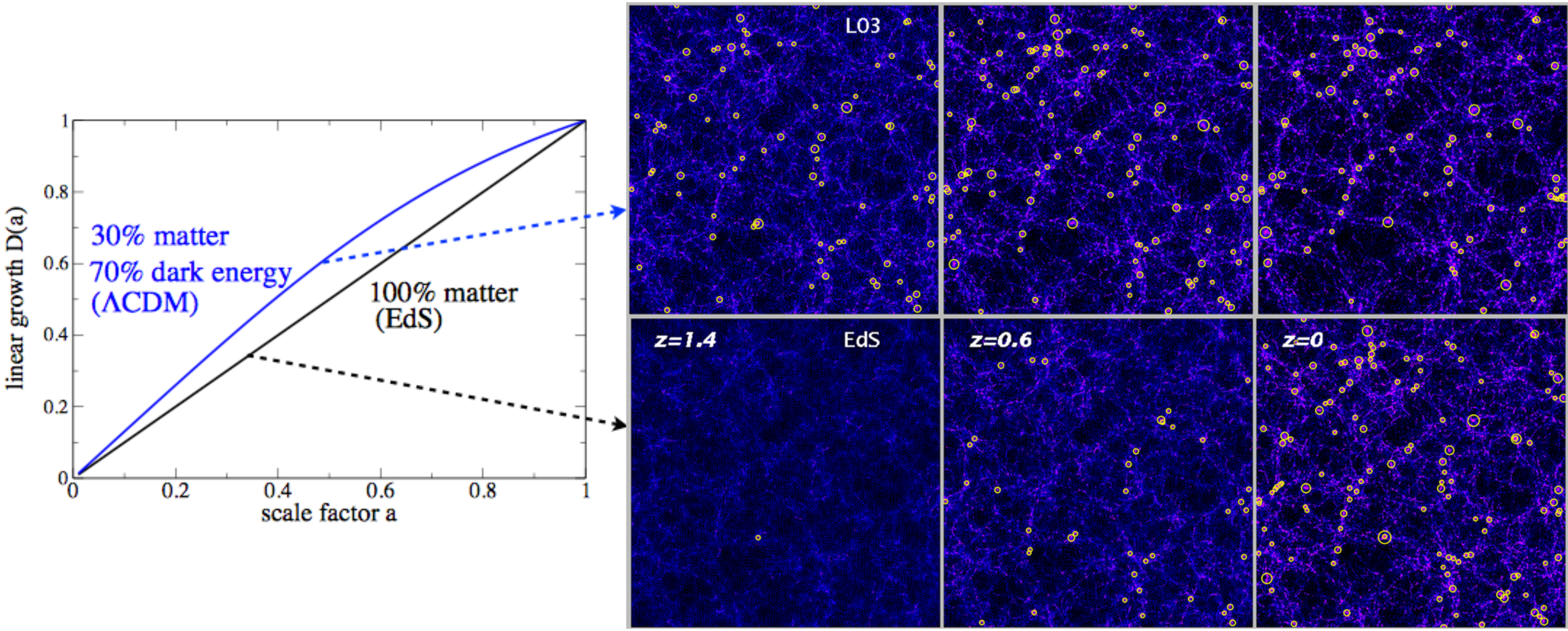

➔ Traced by the evolution of the cluster population

Information from a cluster survey

$$\frac{dN(X;z)}{dXdz} = \frac{dV}{dz} f(X,z) \int_0^\infty \frac{dn(M,z)}{dM} \frac{dp(X|M,z)}{dX} dM$$

→ No. of clusters of given observable X and z within the survey area

Information from a cluster survey

$$\frac{dN(X;z)}{dXdz} = \frac{dV}{dz} f(X,z) \int_0^\infty \frac{dn(M,z)}{dM} \frac{dp(X|M,z)}{dX} dM$$

→ No. of clusters of given observable X and z within the survey area

1. Friedmann background: $\frac{dV}{dz}$ → Priors from CMB, BAO, SN-Ia, ….

Information from a cluster survey

$$\frac{dN(X;z)}{dXdz} = \frac{dV}{dz} f(X,z) \int_0^\infty \frac{dn(M,z)}{dM} \frac{dp(X|M,z)}{dX} dM$$

➔ No. of clusters of given observable X and z within the survey area

1. Friedmann background: $\frac{dV}{dz}$ ➔ Priors from CMB, BAO, SN-Ia, ….
2. Selection function: $f(X,z)$ ➔ Observational strategy

Information from a cluster survey

$$\frac{dN(X;z)}{dXdz} = \frac{dV}{dz} f(X,z) \int_0^\infty \frac{dn(M,z)}{dM} \frac{dp(X|M,z)}{dX} dM$$

➔ No. of clusters of given observable X and z within the survey area

1. Friedmann background: $\frac{dV}{dz}$ ➔ Priors from CMB, BAO, SN-Ia, ….

2. Selection function: $f(X,z)$ ➔ Observational strategy

3. Growth history and nature of perturbations: $\frac{dn(M,z)}{dM}$ ➔ Precisely calibrated with N-body simulations

Information from a cluster survey

$$\frac{dN(X;z)}{dXdz} = \frac{dV}{dz} f(X,z) \int_0^\infty \frac{dn(M,z)}{dM} \frac{dp(X|M,z)}{dX} dM$$

→ No. of clusters of given observable X and z within the survey area

1. Friedmann background: $\frac{dV}{dz}$ → Priors from CMB, BAO, SN-Ia, ….

2. Selection function: $f(X,z)$ → Observational strategy

3. Growth history and nature of perturbations: $\frac{dn(M,z)}{dM}$ → Precisely calibrated with N-body simulations

4. Astrophysics: $p(X|M,z)$ → Priors on "nuisance parameters" p_j from follow-up observations and/or <u>cosmological simulations</u>

Halo Mass Function

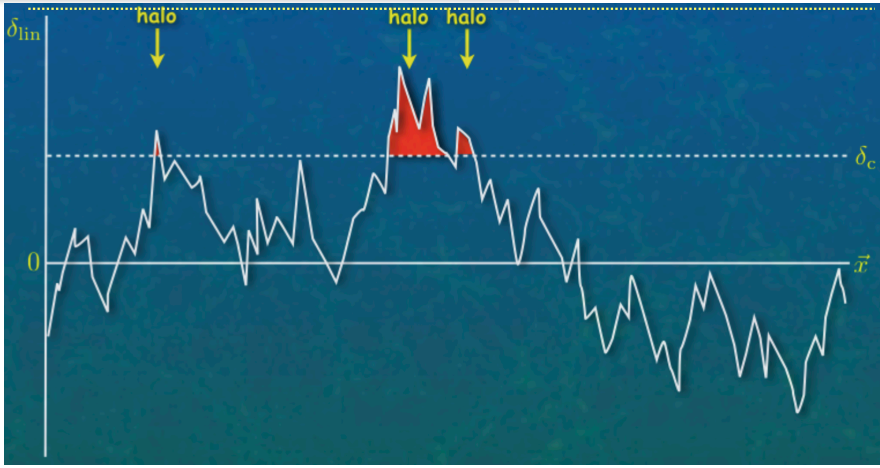

$$n(M,z)dM = \frac{\bar{\rho}}{M^2} f(\nu) \frac{d\ln\nu}{d\ln M} dM$$

$$\nu = \delta_c / \sigma_M(z)$$

δ_c : linear critical density constrast for spherical collapse

$$\sigma_M^2(z) = \frac{D^2(z)}{2\pi^2} \int_0^\infty dk\, k^2 P(k) W_M^2(k)$$

➔ Mass variance at the scale M and redshift z for the filter function $W_M(k)$.

$D(z, k) = D(\Omega_m, \Omega_{DE}, \Omega_\nu, w, \ldots)$: linear growth rate of density fluctuations

$$\nu f(\nu) = \left(\frac{\nu}{2\pi}\right)^{1/2} e^{-\nu/2}$$

➔ Press & Schechter 74

$$\nu f(\nu) = A\left[1 + \frac{1}{(a\nu)^p}\right]\left(\frac{a\nu}{2\pi}\right)^{1/2} e^{-a\nu/2}$$

➔ Sheth & Tormen 99

(A, a, p): fitting parameters from N-body

Cluster Cosmology ~20 yrs ago

SB et al. ’01; Rosati, SB & Norman ‘02

- ~100 clusters identified from ROSAT PSPC pointings
- Only X-ray luminosity available

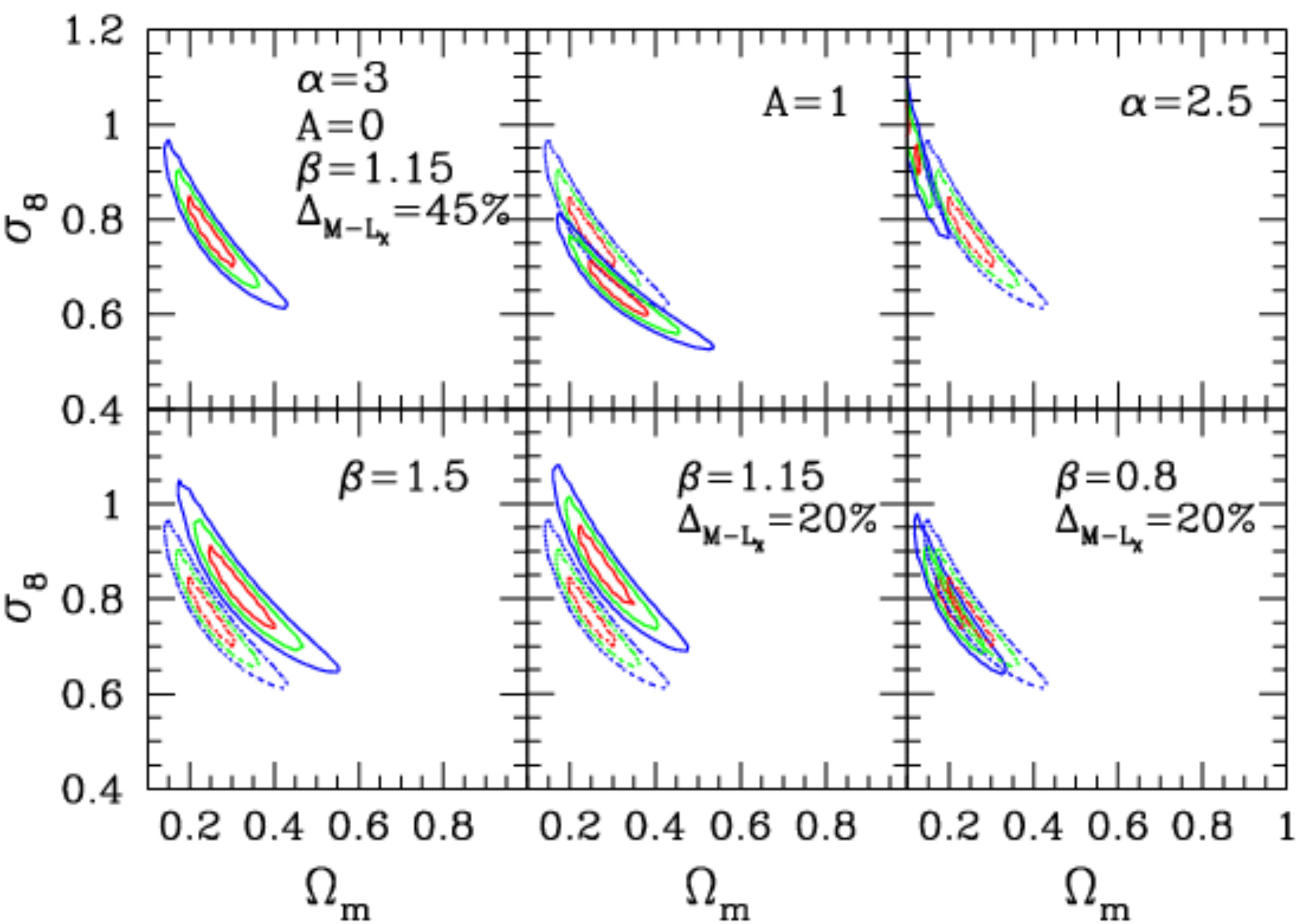

- Ω_m<0.6 at >3σ
- σ_8 = 0.75 ± 0.05 (Ω_m = 0.27) for the reference analysis
- Results dependent on ICM physics....

Planck CMB & clusters

Planck collab. 2013 XX

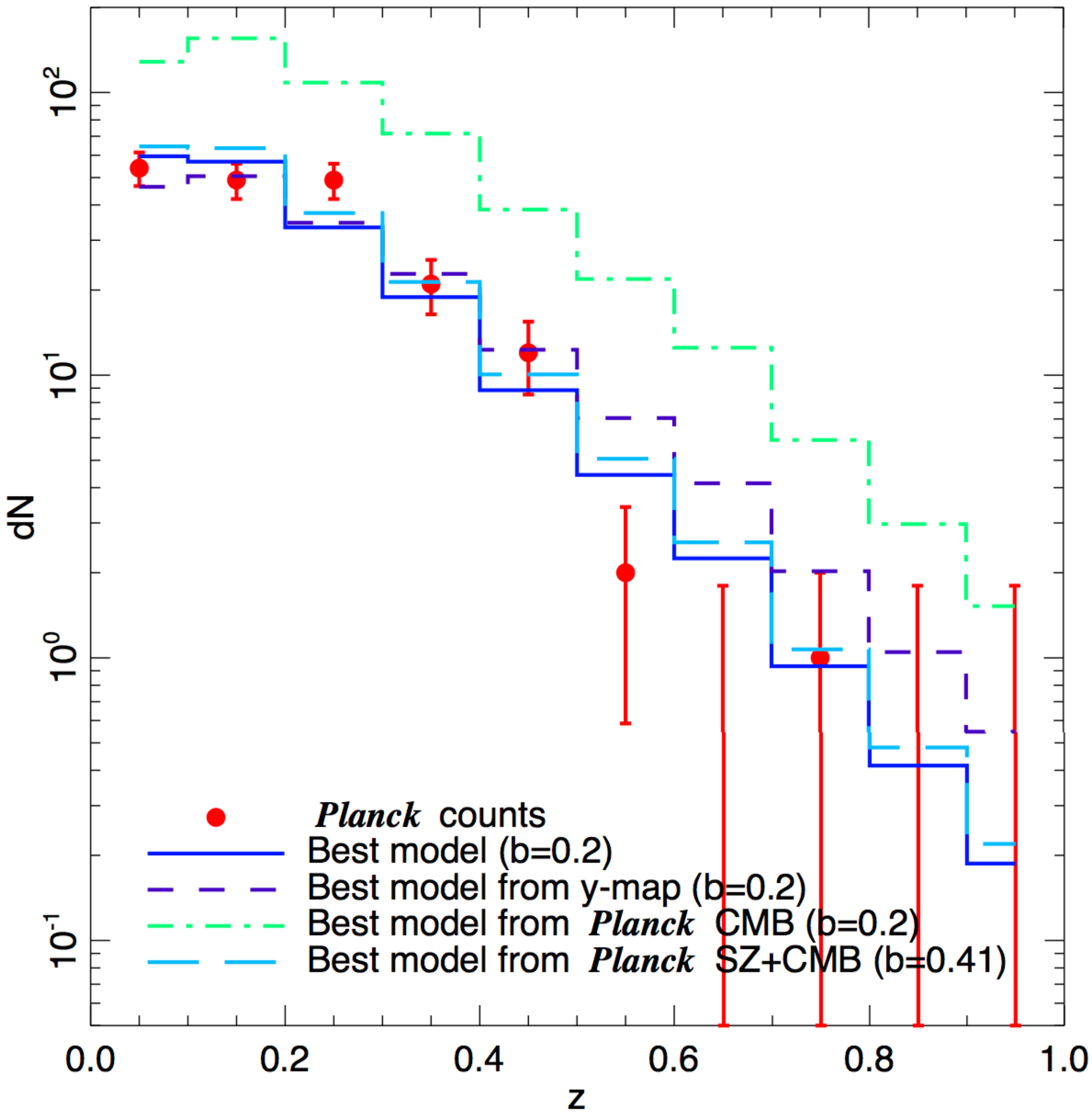

Number counts for 189 Planck-SZ clusters

➔X-ray (XMM) calibrated mass scaling

➔Tension with Planck primary CMB

➔**b=0.2** (HE mass bias)**:** suggested by simulations

➔Agreement with constraints from:

- Planck-y map
- Other cluster counts
- Cosmic shear

Cluster cosmology as of today

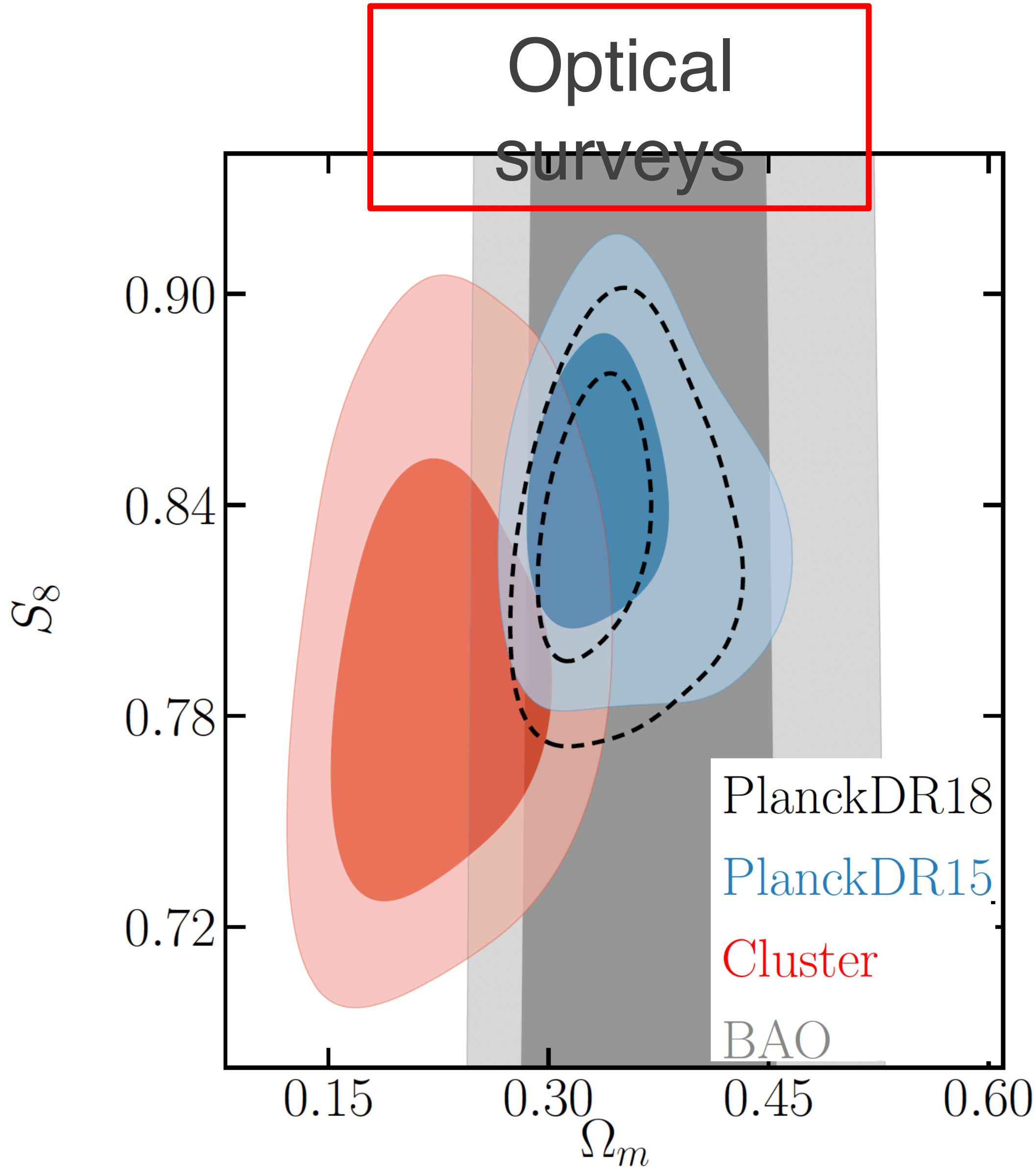

Costanzi+2018: abundance and weak-lensing of RedMapper clusters from SDSS (z=0.1-0.3)

➔ ~7000 clusters used

$$S_8 \equiv \sigma_8(\Omega_m/0.3)^{0.5} = 0.79^{+0.05}_{-0.04}.$$

➔ No evidence of tension with CMB constraints and constraints from other cluster catalogues

Cluster cosmology as of today

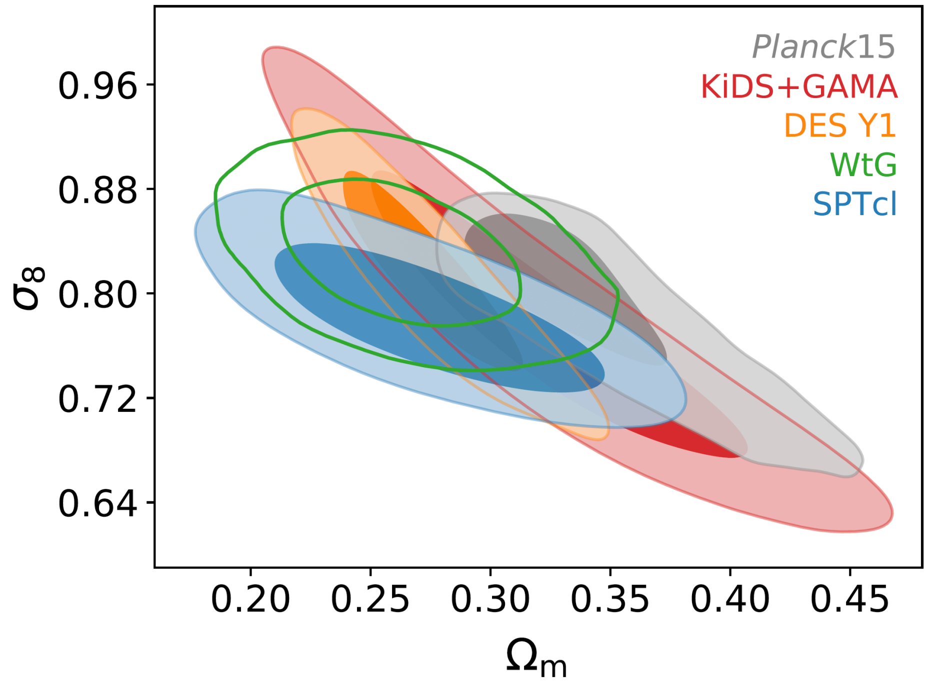

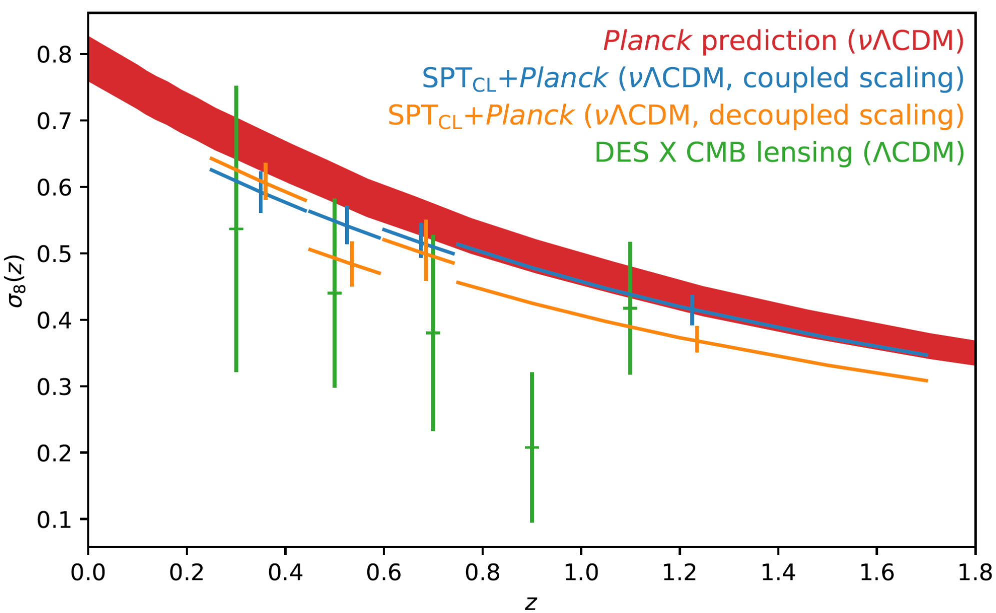

SZ surveys

Bocquet+2018: cluster counts in the SPT-SZ survey (z=0.25-1.75)

- ➔ 377 clusters used, supplemented by HST+Magellan WL mass and Chandra X-ray observations
- ➔ Allow neutrino mass to be a free
- ➔

$$\Omega_m = 0.276 \pm 0.047$$
$$\sigma_8 = 0.781 \pm 0.037$$

- ➔ Test of growth of structure in agreement with GR

Part II:
Simulations for cluster cosmology

What simulations are used for?

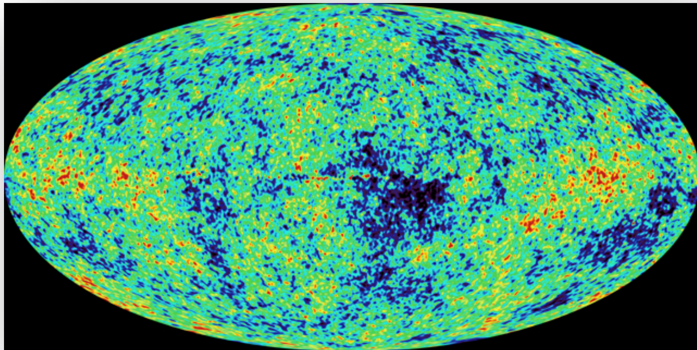

- ➔ Evolve cosmic structures from initial conditions set by CMB observations

Why simulations of clusters?

- ➔ Impact of astrophysical processes in determining the observational properties of clusters
- ➔ Understand systematics and biases in the calibration of clusters as tools for cosmology

What simulations are used for?

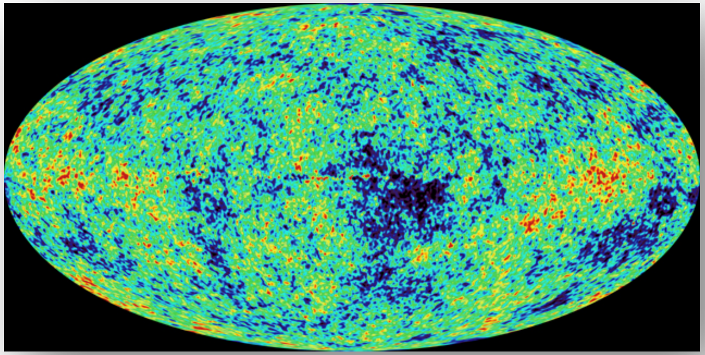

→ Evolve cosmic structures from initial conditions set by CMB observations

Why simulations of clusters?

→ Impact of astrophysical processes in determining the observational properties of clusters

→ Understand systematics and biases in the calibration of clusters as tools for cosmology

What simulations are used for?

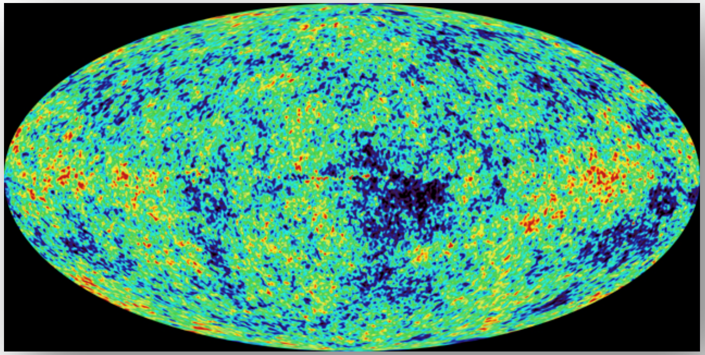

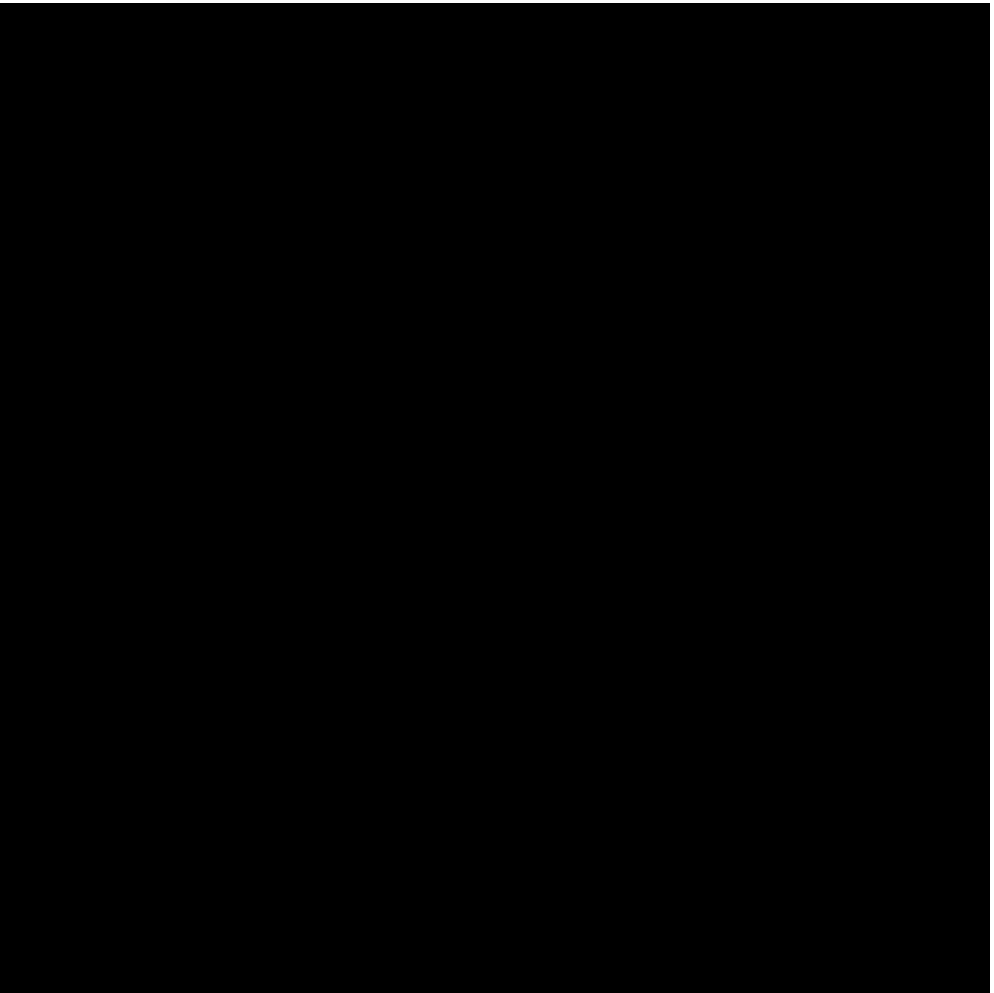

➔ Evolve cosmic structures from initial conditions set by CMB observations

Why simulations of clusters?

➔ Impact of astrophysical processes in determining the observational properties of clusters

➔ Understand systematics and biases in the calibration of clusters as tools for cosmology

Large-scale hydrodynamic simulations

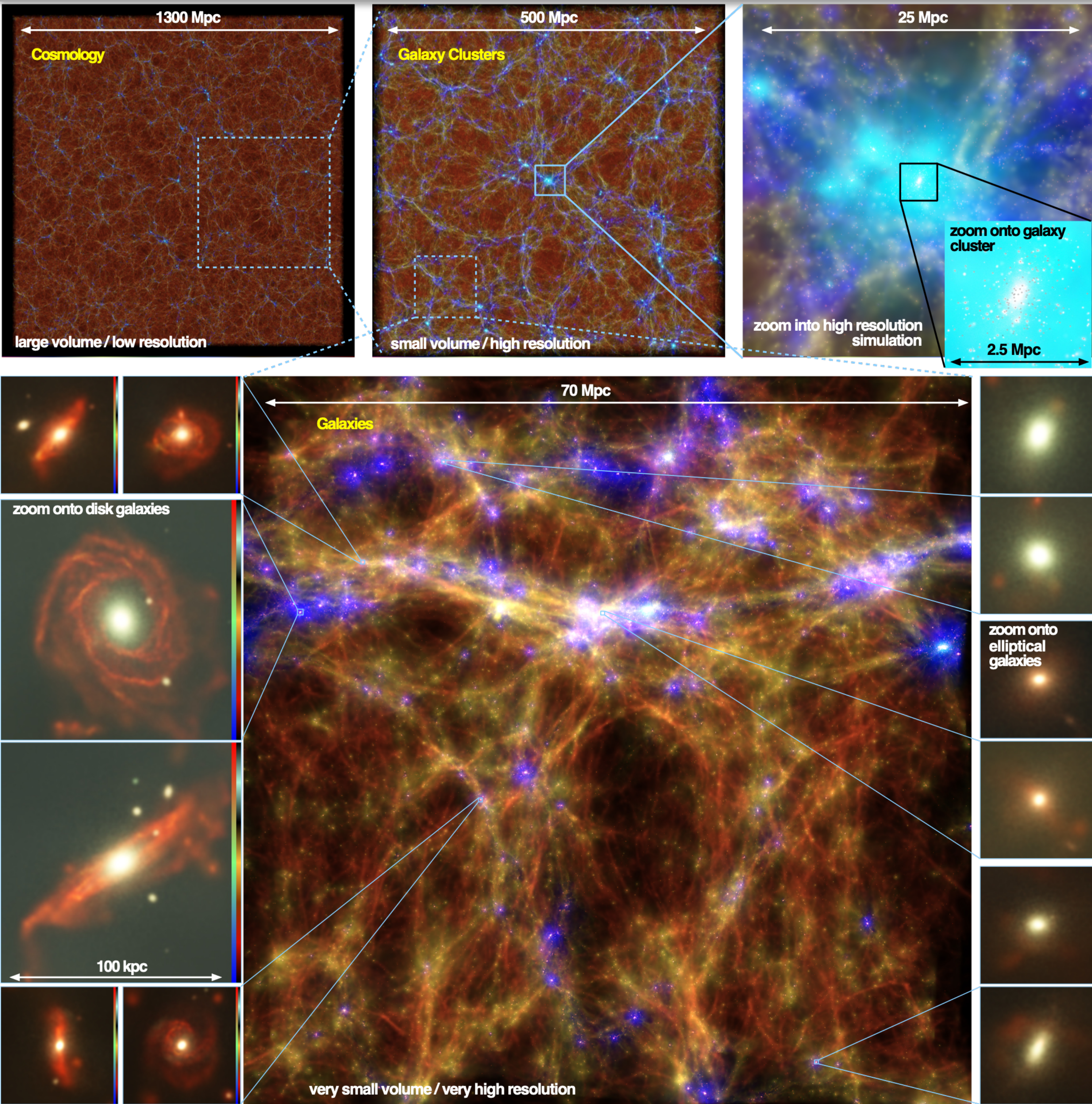

"Magneticum"
Dolag+2015
www.magneticum.org

"Illustris-TNG300"
Vogelsberger+2017
www.tng-project.org

"Bahamas"
McCarthy+2017
http://www.astro.ljmu.ac.uk/~igm/BAHAMAS/

"Horizon"
https://www.horizon-simulation.org

Zoom-in simulations

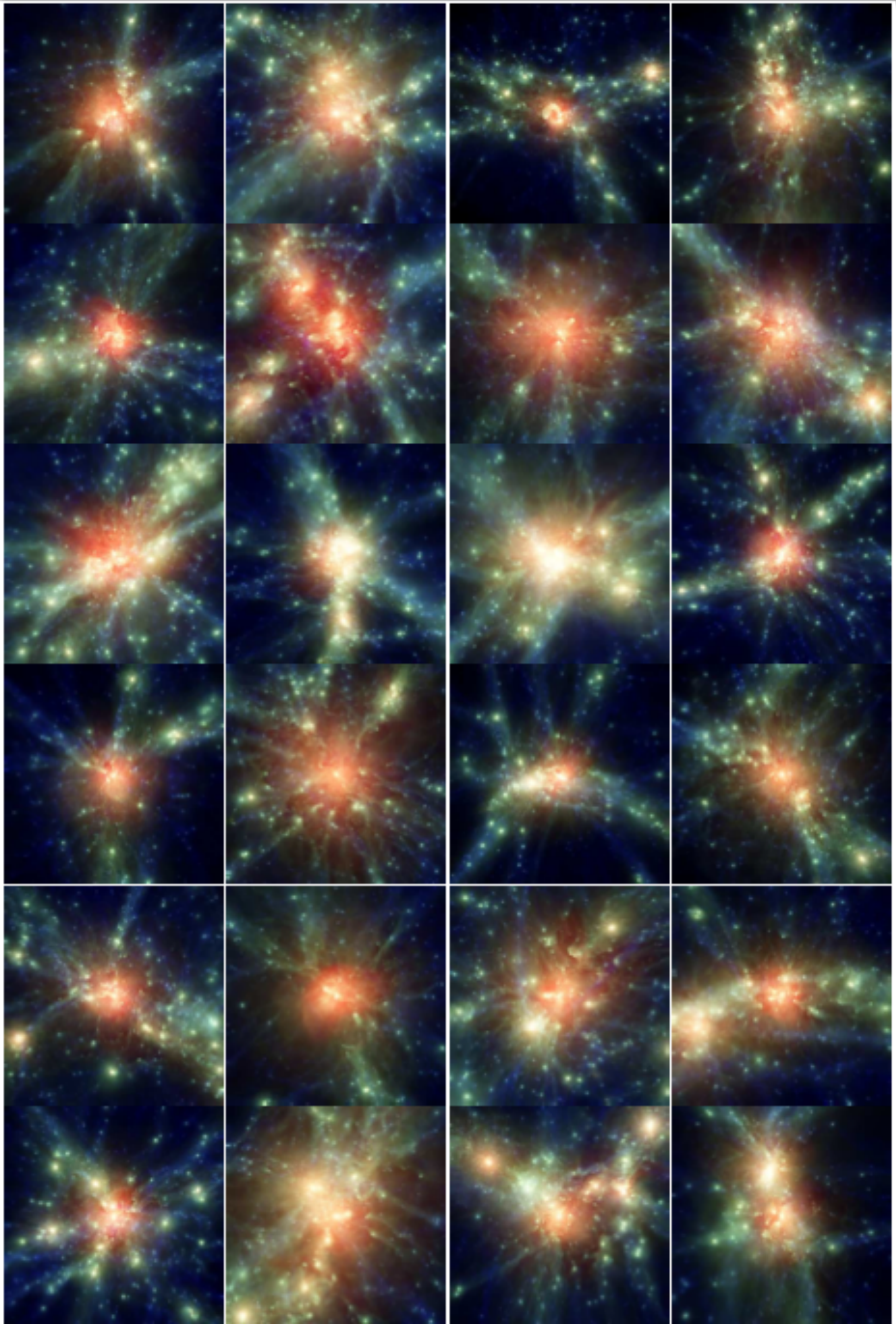

→ **Dianoga simulations**
Rasia et al. 2015

→ **“The 300” project**
Cui et al. 2018

→ **MACSIS simulations**
Barnes et al. 2017

→ **Hydrangea/C-EAGLE**
Bahè et al. 2018

→ **FABLE**
Henden et al. 2019

Zoom-in simulations

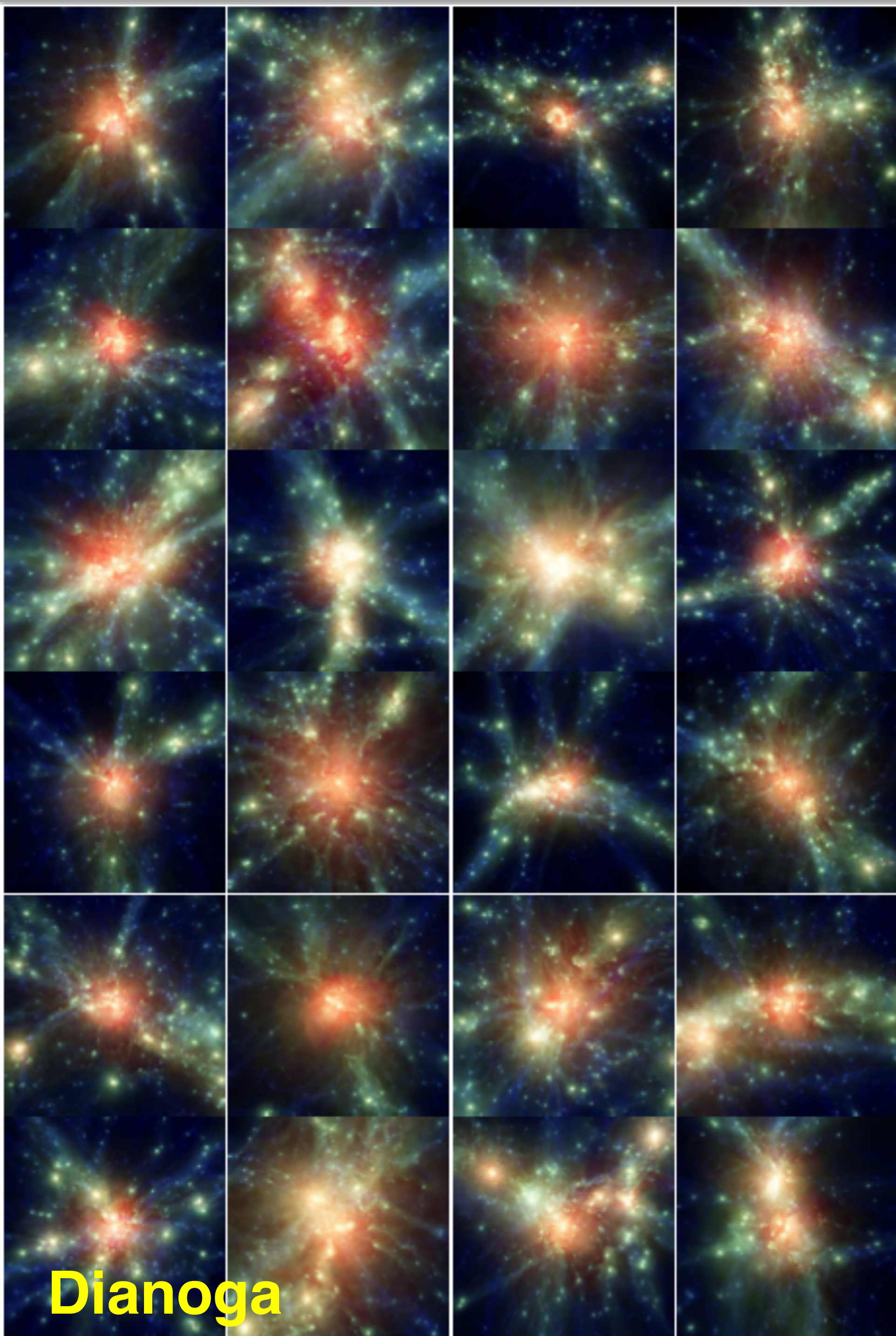

- 140 halos with M_{vir}>5 x 10^{13} h^{-1} $M_{\odot}$

- Hydro (Beck+15): Gadget-3 SPH +
  - Higher-order kernel
  - “Wake-up” scheme for time-step of gas particles
  - Time-dependent artificial viscosity
  - Artificial conduction

- Astrophysics:
  - Cooling + SF + SN feedback (Springel & Hernquist 03)
  - Chemical enrichment (Tornatore+07)
  - AGN feedback (Steinborn+15)

BH scaling relations

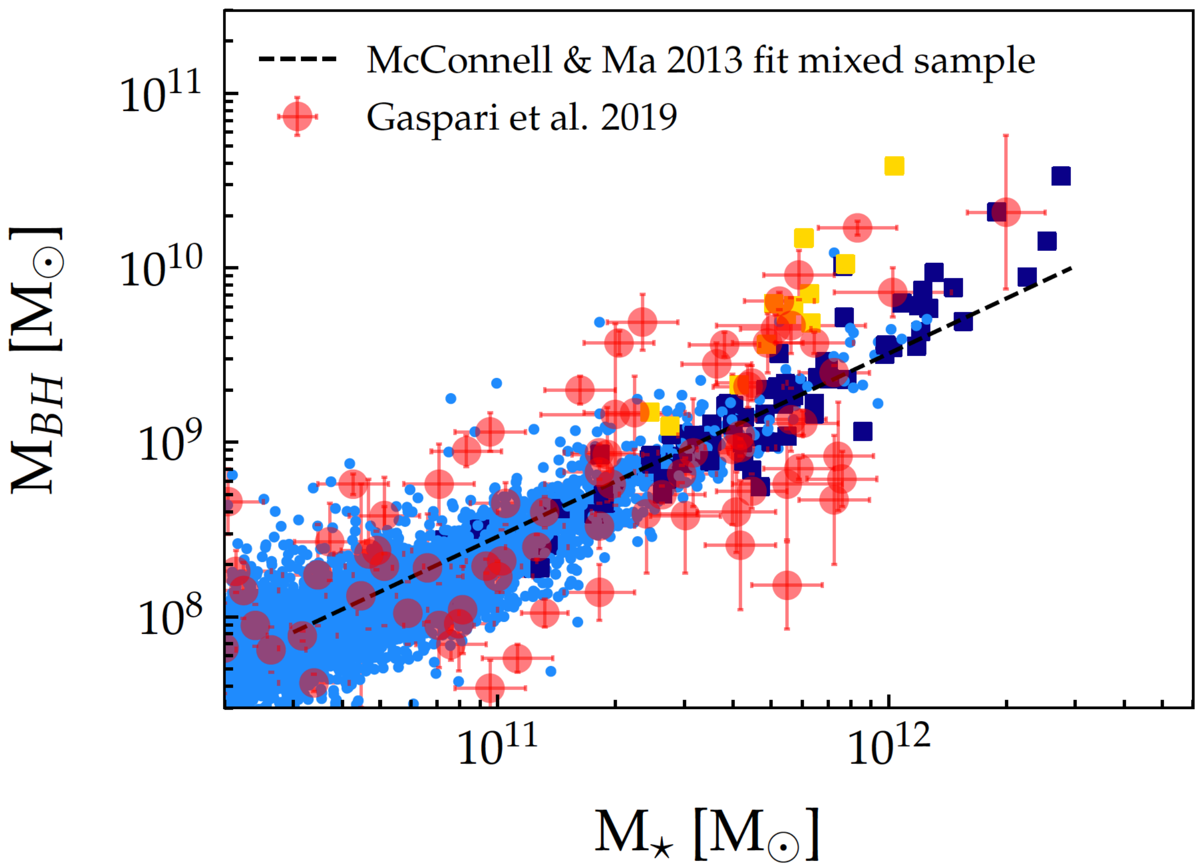

Bassini+19

Bassini+20 ; in prep

➔M_{BH}-M_* relation to calibrate feedback parameters

Observations from:

McConnell & Ma 2013

Main+2017 (M_{BH} from K-band luminosity)

BH scaling relations

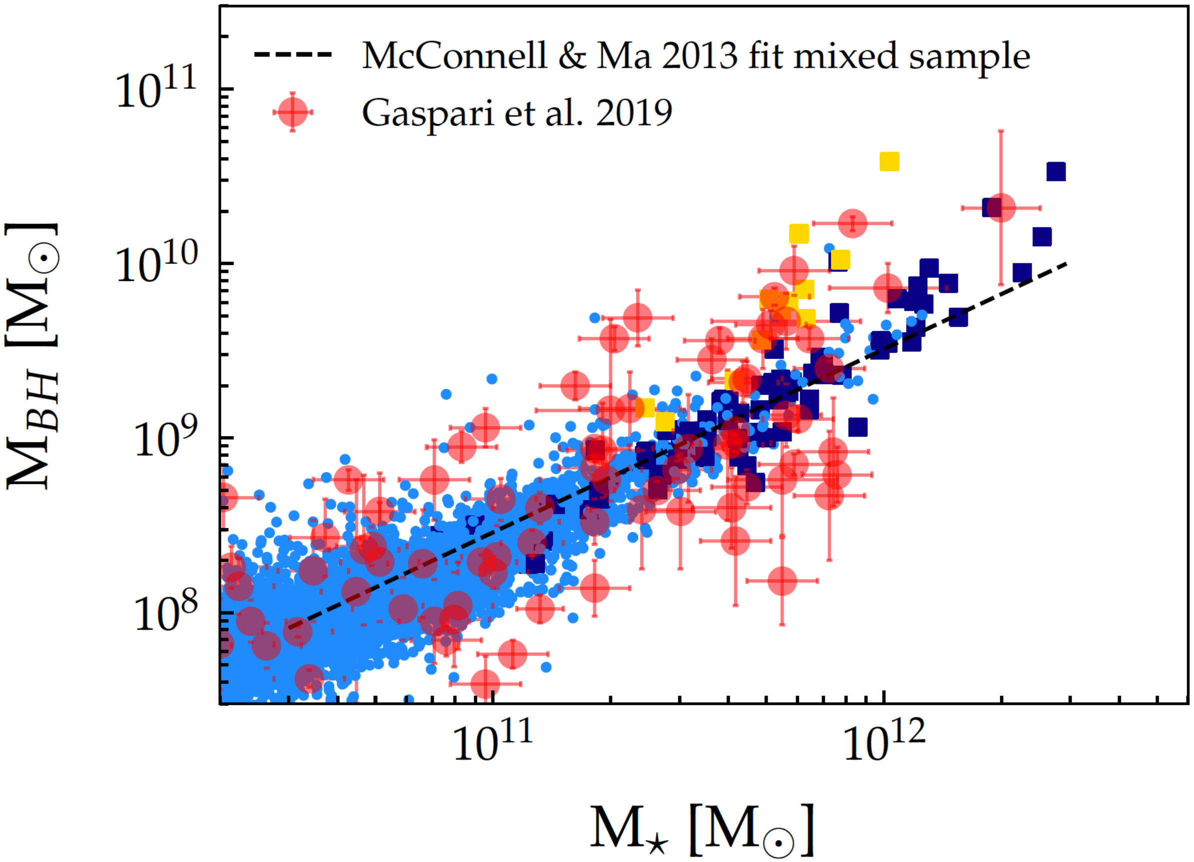

Bassini+19

Bassini+20 ; in prep

➔M_{BH}-M_* relation to calibrate feedback parameters

Observations from: McConnell & Ma 2013 Main+2017 (M_{BH} from K-band luminosity)

➔Relationship with general ICM properties (temperature) also reproduced

Observations from: Gaspari+2019

BH scaling relations

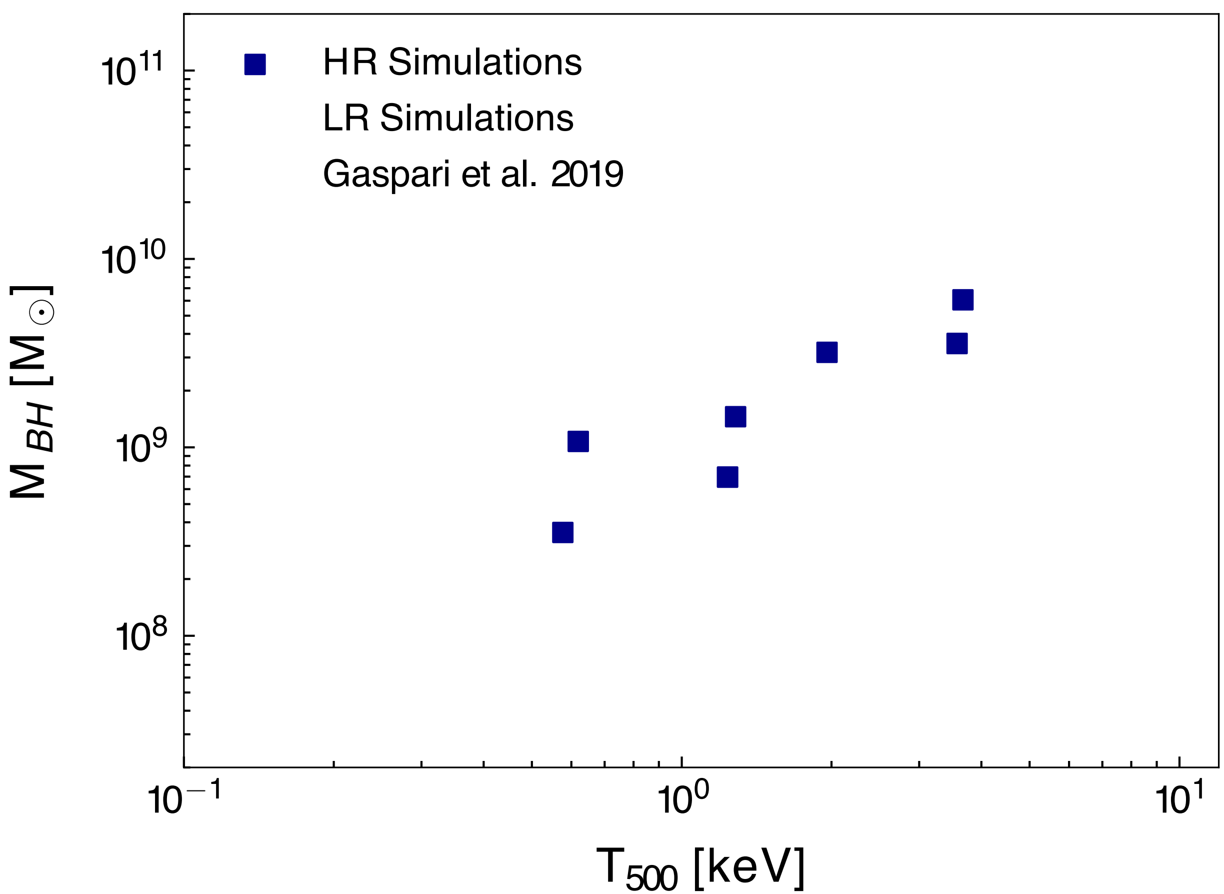

Bassini+19

Bassini+20 ; in prep

➔M_{BH}-M_* relation to calibrate feedback parameters

Observations from:

McConnell & Ma 2013

Main+2017 (M_{BH} from K-band luminosity)

➔Relationship with general ICM properties (temperature) also reproduced

Observations from:

Gaspari+2019

Part II.a:
Calibration of the Halo Mass Function

Calibration of halo mass function

E.g. for ΛCDM: Sheth & Tormen 2001, Jenkins+2001, Evrard+2002, Springel+2005, Warren+2007, Reed+2007, Tinker+2008, Crocce+2010, Courtin+2011, Bhattacharya+2011, Angulo+2012, Watson+2013, Despali+2016, ...

What is a universal HMF?

$$n(M,z)\,dM = \frac{\bar{\rho}}{M^2}\, f(\nu)\, \frac{d\ln\nu}{d\ln M}\, dM$$

$$\nu = \delta_c / \sigma_M(z)$$

- Functional form of $f(\nu)$ independent of cosmology
- Cosmology entering only through $\nu(M,z)$

Why calibrating a universal HMF?

- Much easier to sample parameter space of cosmological models
- No need to carry out brute-force calibration with N-body simulations when changing cosmology

Violation of universality ....

Tinker+2008

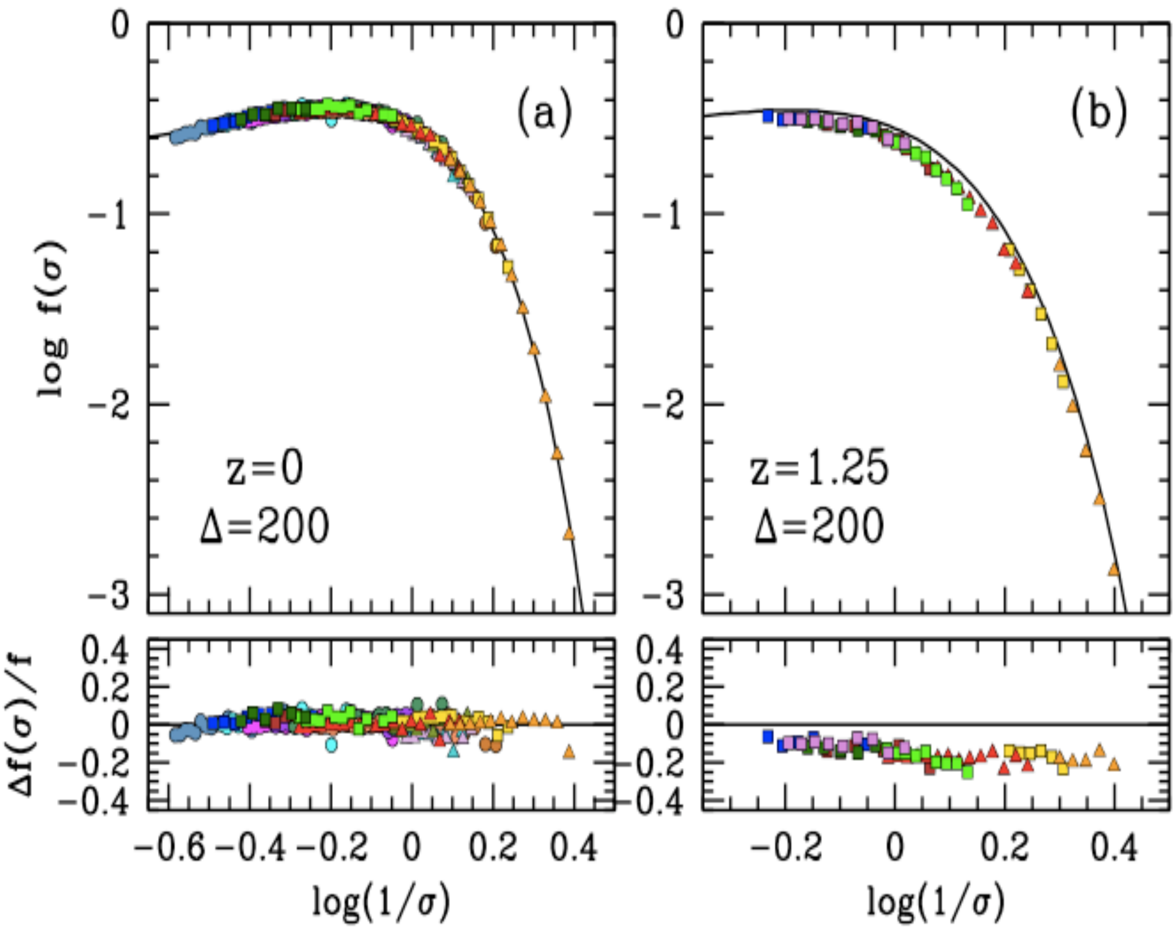

➔ HMF from several simulations of WMAP1 and WMAP3 cosmologies

➔ SO halo finder at several values of overdensity *Δ* (in units of mean cosmic density)

Main result: significant violation of universality, whose amount depends on halo mass definition

Q1: can such a lack of universality be calibrated?

Q2: should this be surprising?

.... or maybe not

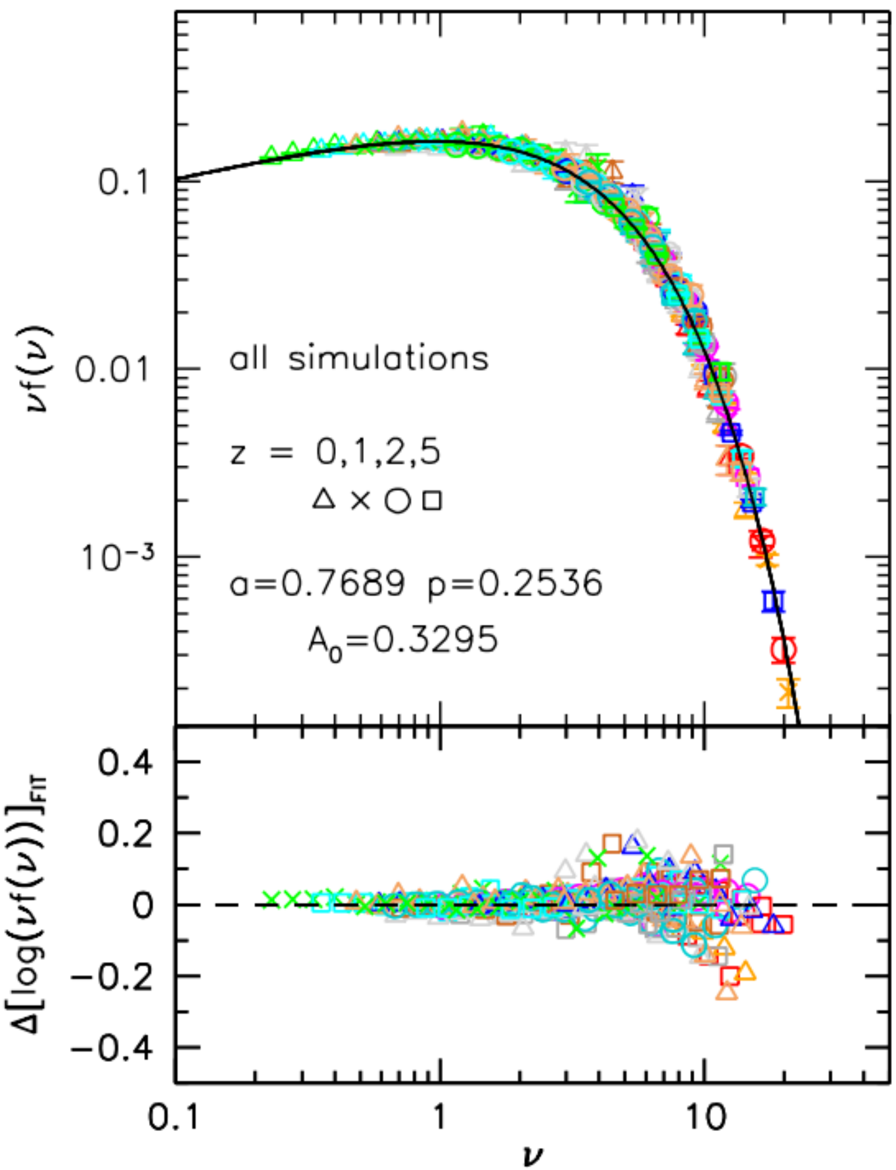

Despali+2016

- Homogeneous set of simulations of Planck-concordance cosmology
- Universality expected to hold when using the redshift- and cosmology-dependent values of Δ predicted by spherical collapse

➔ HMF consistent with being universal within 10%

Q1: Is universality preserved for beyond-ΛCDM cosmologies?

Q2: Is it accurate enough for the

Towards a universal HMF

Planck cosmology

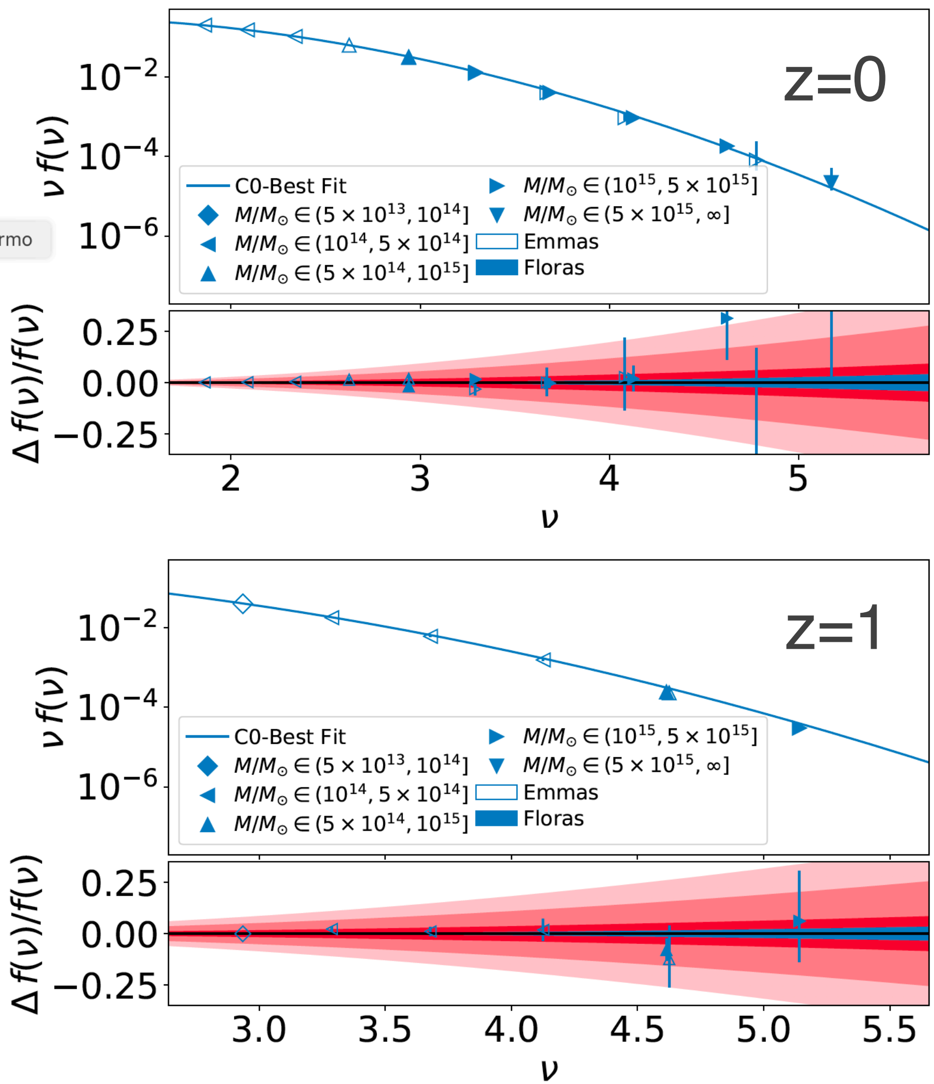

Castro+2020a in prep

- Large suite of N-body simulations with 1024^3 particles for Planck cosmology + 2 more cosmologies:
  - 11 x 1 h^{-1} Gpc boxes
  - 11 x 2 h^{-1} Gpc boxes

➔ **Total of ~66 boxes**

➔ Sheth+2001 fitting function

$$\nu f(\nu) = 2\,A\left(1 + \frac{1}{\nu'^{2p}}\right)\left(\frac{\nu'^2}{2\pi}\right)^{1/2} \exp\left(-\frac{\nu'^2}{2}\right)$$

$$\nu' = a_0\,\Omega_m(z)^{a_z}\,\nu \qquad \nu(z) \equiv \frac{\delta_c(z)}{\sigma_M(z)}$$

➔ HMF consistent with being universal within ~1%

➔ Subdominant wrt propagated uncertainties in WL mass

Effects of baryons on the HMF

Cui+2015

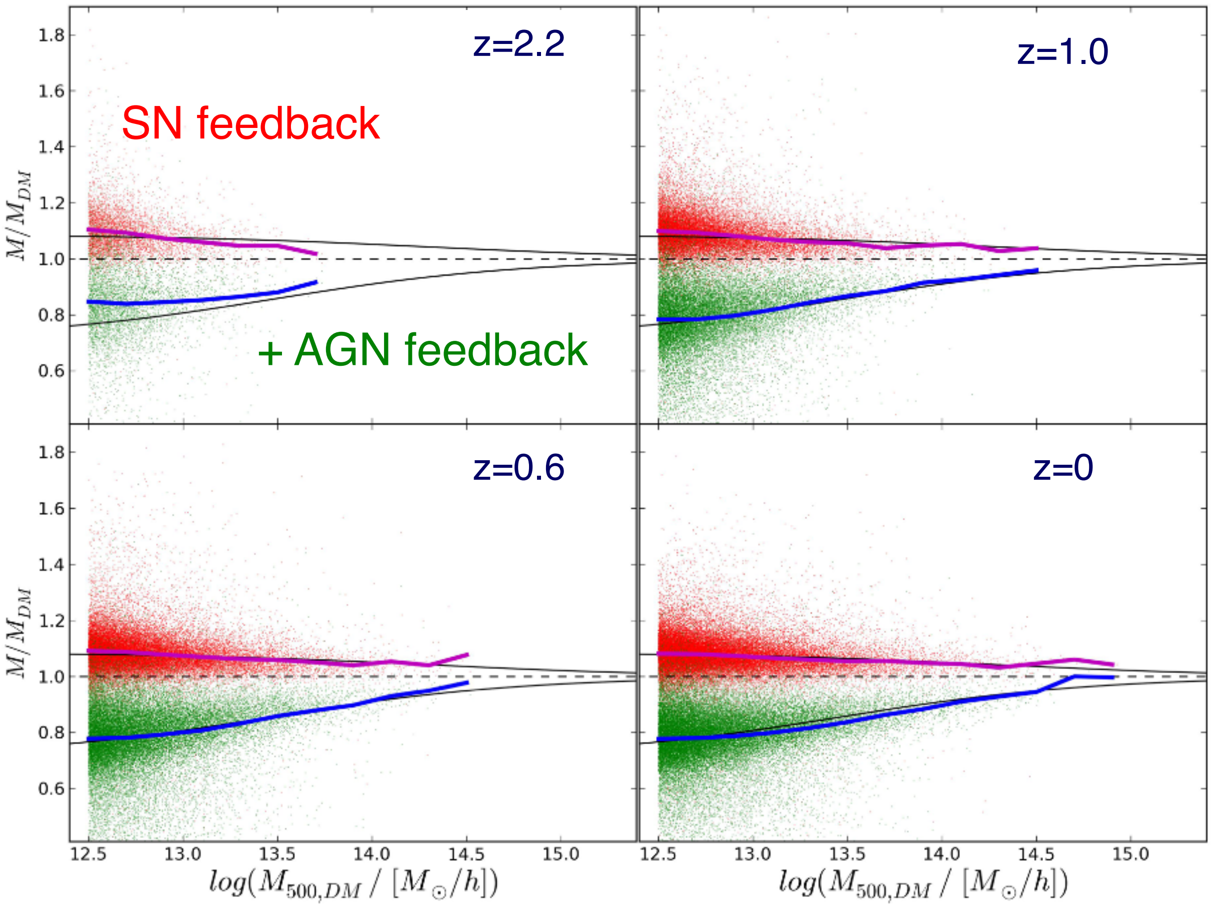

- ➔ Opposite effects for CSF and AGN simulations
- ➔ AGN: ~20% decrease at M_{500}=dex(13.5) h^{-1} $M_\odot$
- ➔ Independent of redshift

Q1: what's the impact on cosmological constraints?

Q2: how robust is the calibration of the baryon effects on halo masses?

Effects of baryons on the HMF

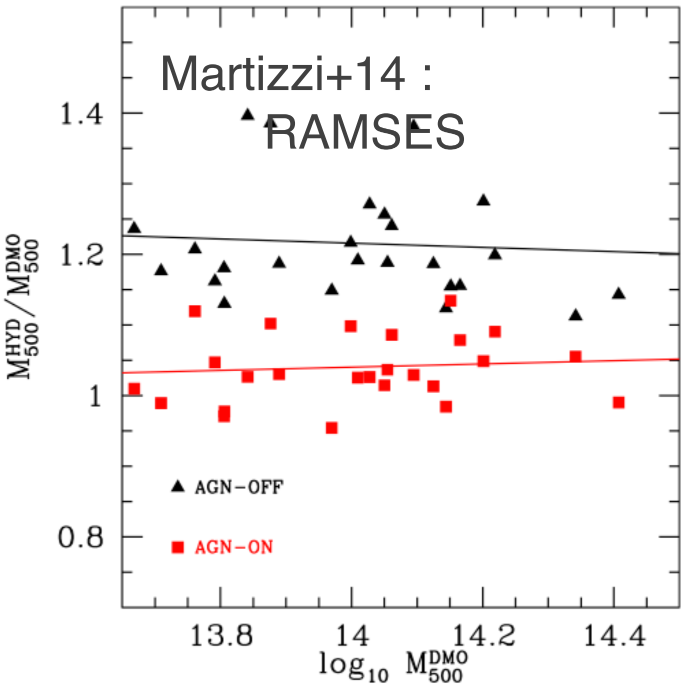

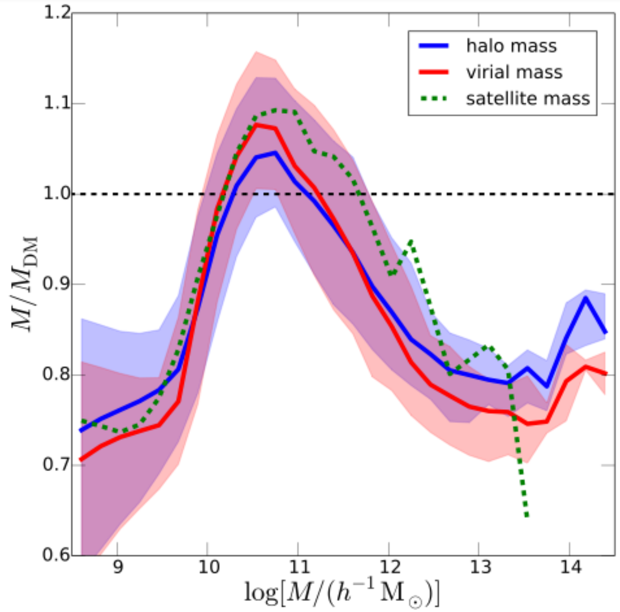

Vogelsberger+14 : AREPO

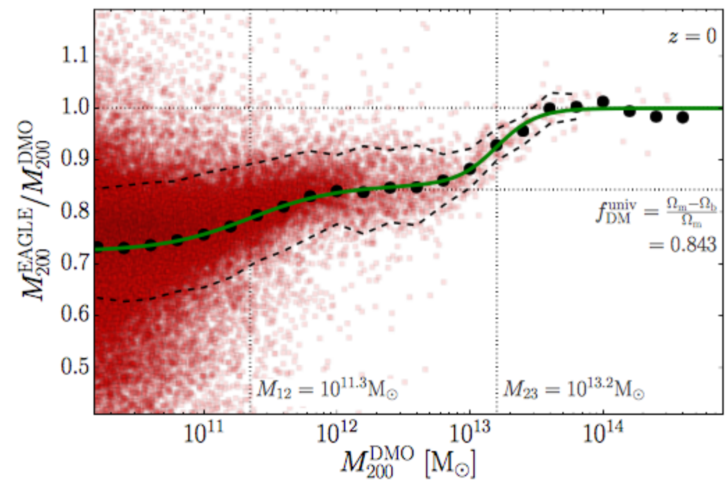

Schaller+14: GADGET-3 (Eagle)

Velliscig+15 : GADGET-3 (OWLS)

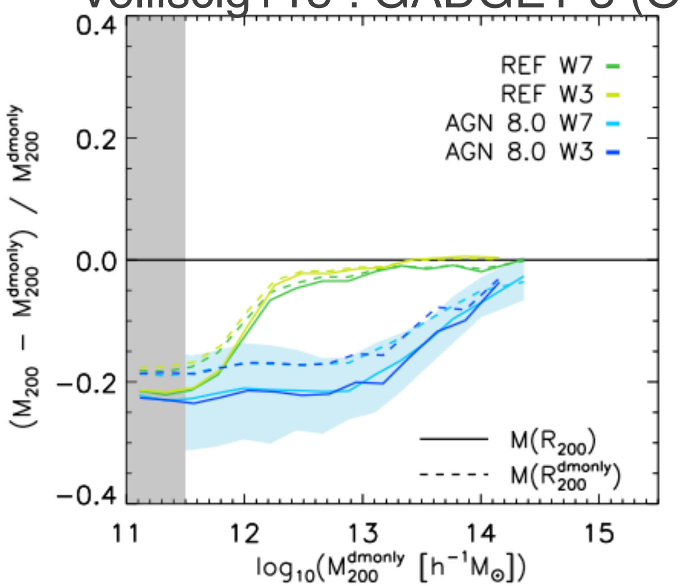

Bocquet+16 : GADGET-3 (Magneticum)

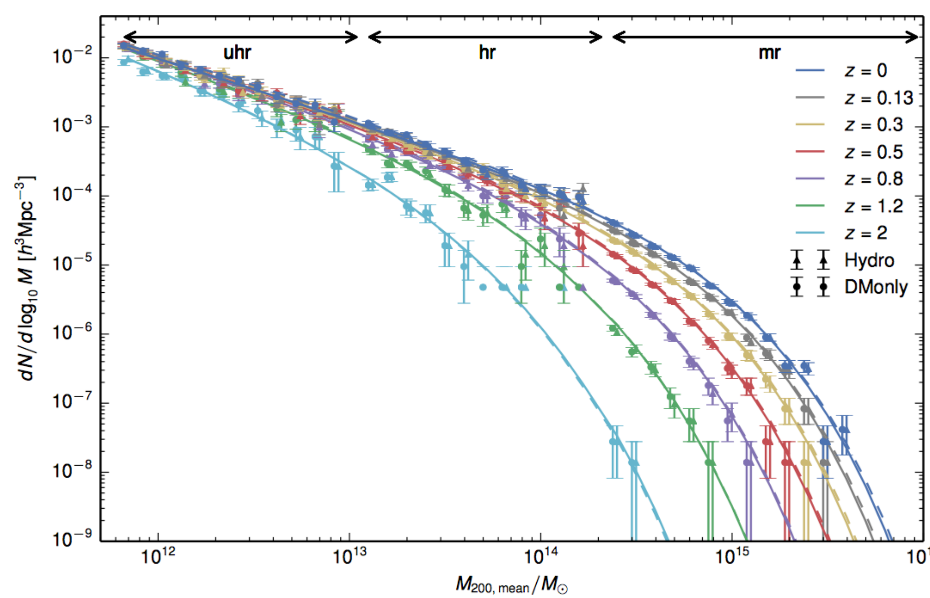

Impact on cosmological constraints

Costanzi+14

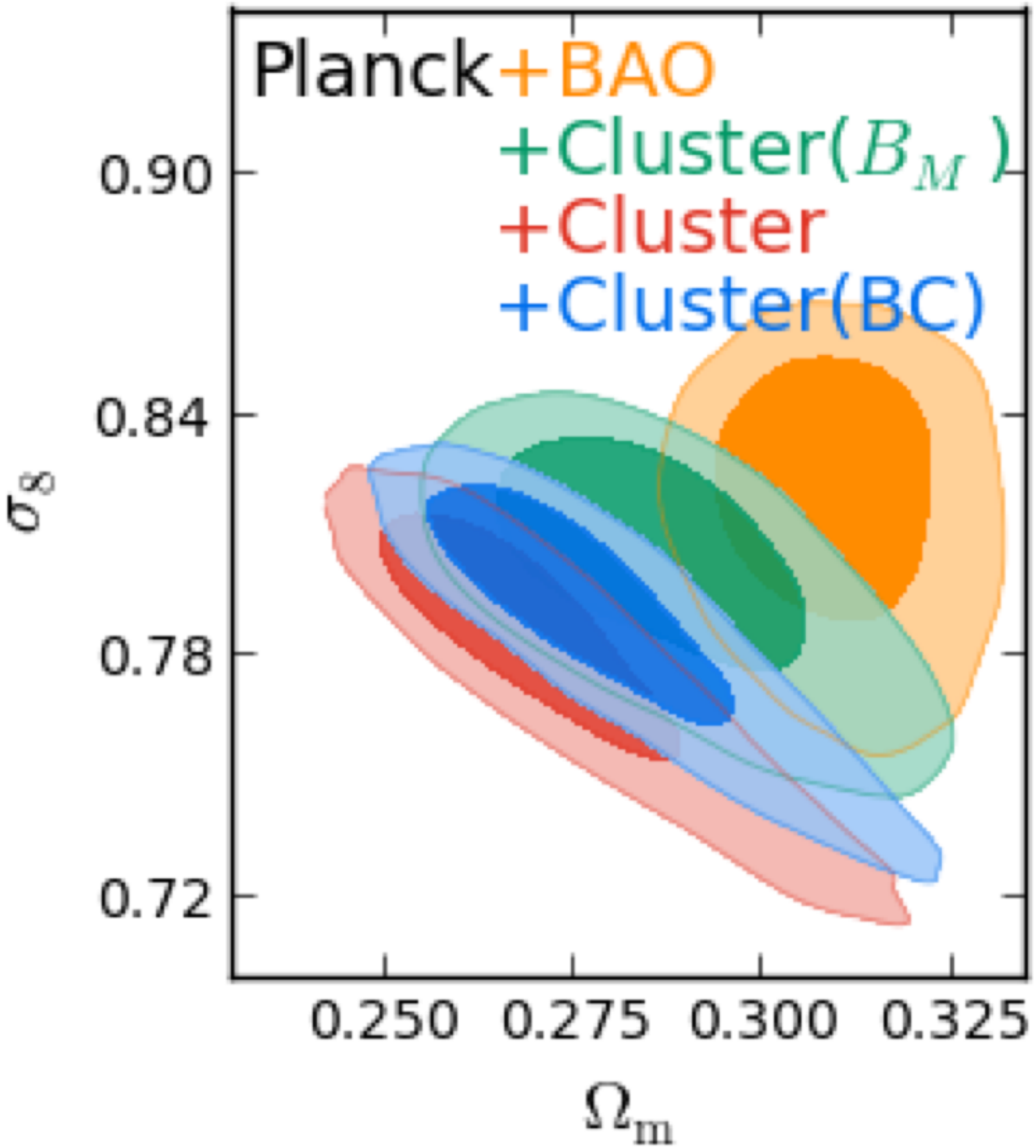

- ➔ Planck CMB
- ➔ BAO from SDSS-DR11 (Anderson+14)
- ➔ CCCP clusters (Vikhlinin+09)
- ➔ Massive neutrinos included

B_M: mass bias = [0.8-1]

BC: HMF baryonic correction

- ➔ Alleviate tension with Planck CMB
- ➔ Crucial to calibrate for future surveys

Baryonic effects on the HMF

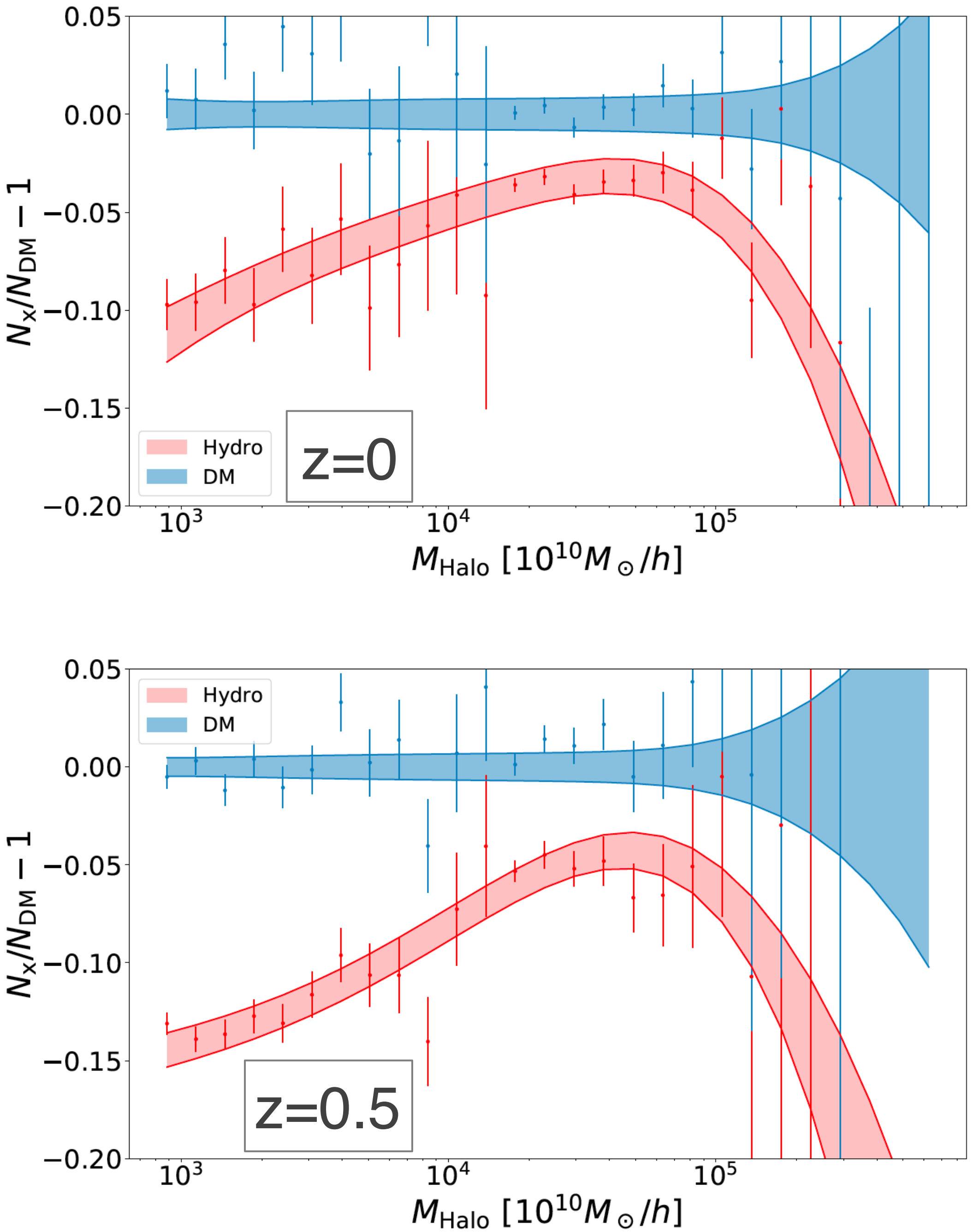

Castro+2020b in prep

- Use the suite of "Magneticum" large-scale hydro simulations
- Fit to a universal Tinker-like HMF with more degrees of freedom to account for baryonic effects
- Non negligible effects on the HMF
- Larger than statistical uncertainties from future (e.g. Euclid) cluster surveys

Part II.b:
Biases in Mass Measurements

Masses from hydrostatic equilibrium

➔ Cosmological simulations to test the accuracy of hydrostatic equilibrium in clusters
(e.g. Rasia+06,12, Nagai+07, Morandi+07, Piffaretti & Valdarnini 08, Meneghetti+09, Lau+09,13, Kay+11, Suto+13, Biffi+16, Pearce+19, Ansarifard+20)

$$\nabla P_{gas} = -\rho_{gas} \nabla \Phi$$

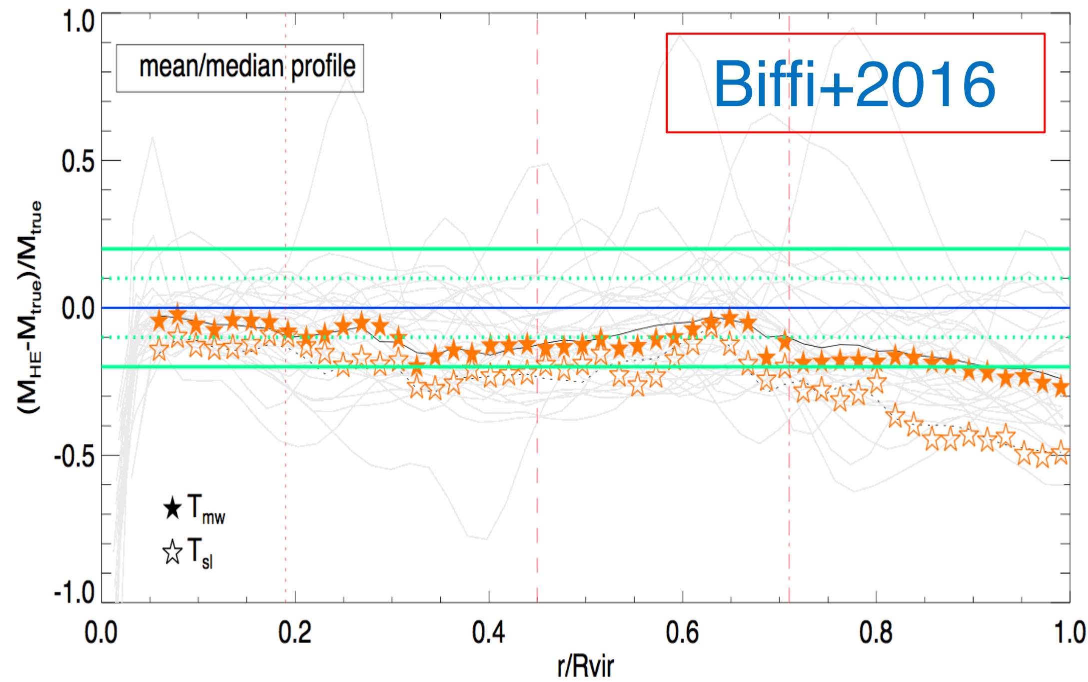

General consensus: 10-20% underestimate of true masses from HE, depending on the cluster dynamical status

Origins of the bias:
1. Non-thermal motions generating a non-thermal pressure support
2. Acceleration term in the Euler equation

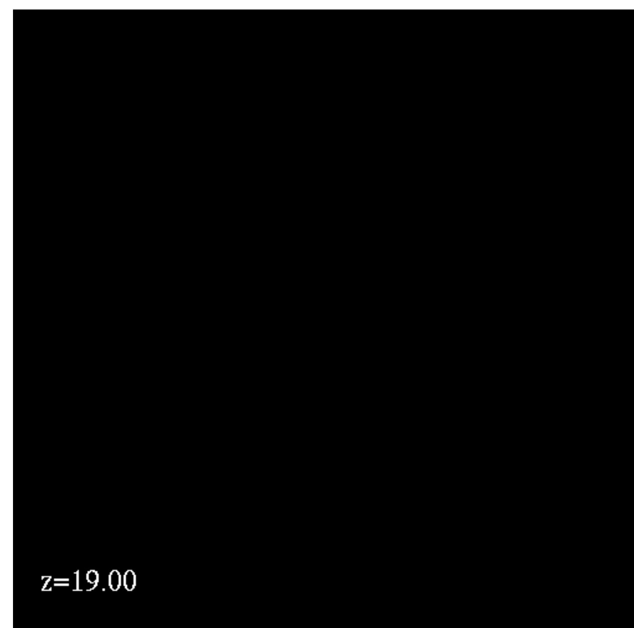

Masses from hydrostatic

→ Cosmological simulations to test the accuracy of hydrostatic equilibrium in clusters
(e.g. Rasia+06,12, Nagai+07, Morandi+07, Piffaretti & Valdarnini 08, Meneghetti+09, Lau+09,13, Kay+11, Suto+13, Biffi+16, Pearce+19, Ansarifard+20)

$$\nabla P_{gas} = -\rho_{gas} \nabla \Phi$$

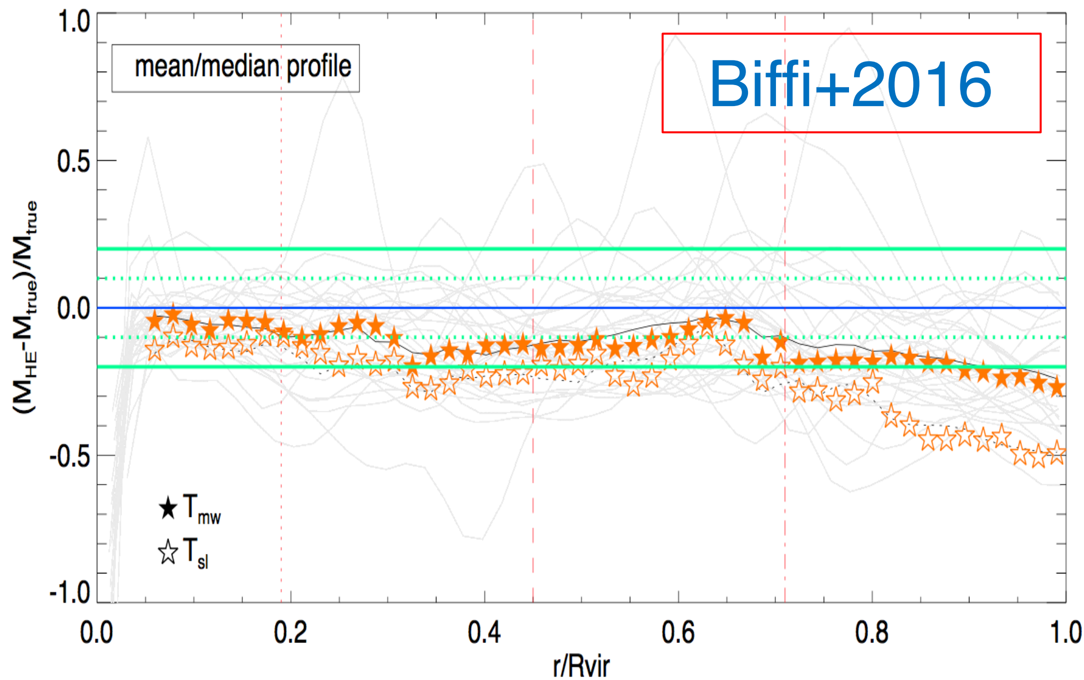

General consensus: 10-20% underestimate of true masses from HE, depending on the cluster dynamical status

Origins of the bias:

1. Non-thermal motions generating a non-thermal pressure support
2. Acceleration term in the Euler equation

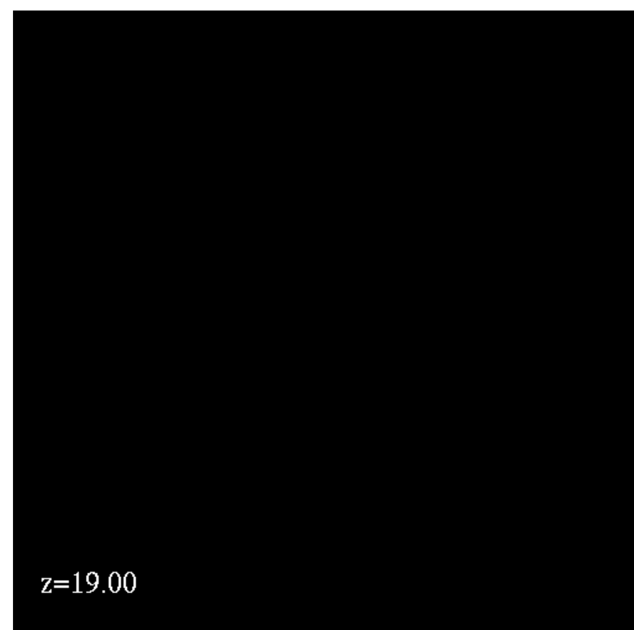

X-ray temperature bias

Q: What's the temperature measured from an X-ray spectrum for a plasma which is not single temperature? (Mazzotta+2004; Vikhlinin 2006)

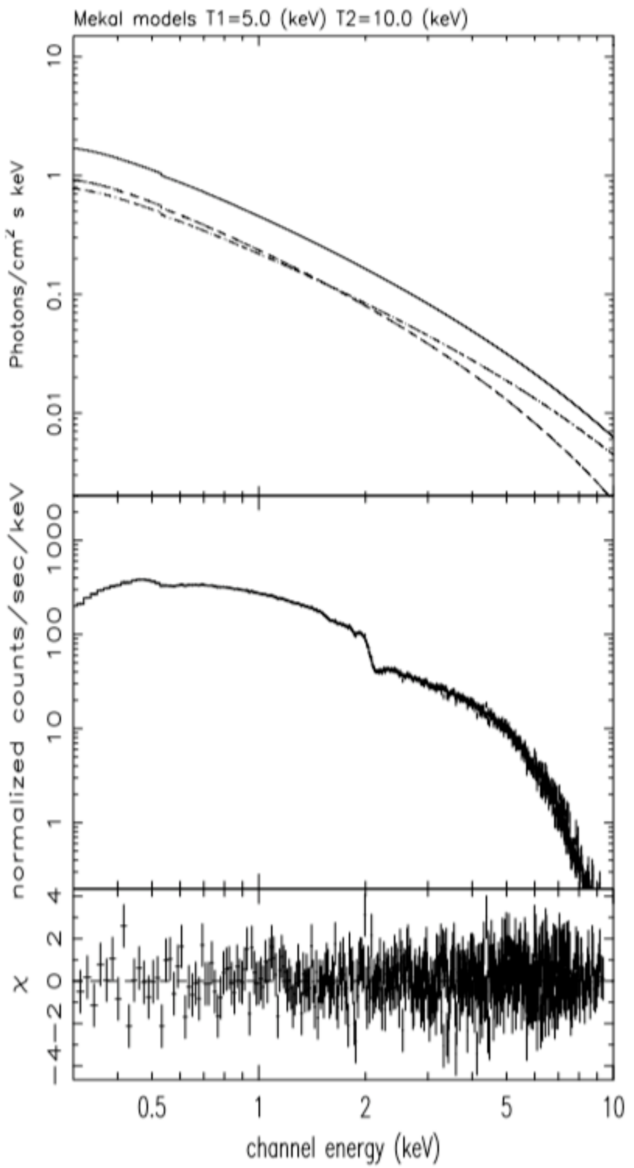

X-ray temperature bias

Q: What's the temperature measured from an X-ray spectrum for a plasma which is not single temperature? (Mazzotta+2004; Vikhlinin 2006)

→ In realistic conditions, single-T model still a good fit to a multi-T model

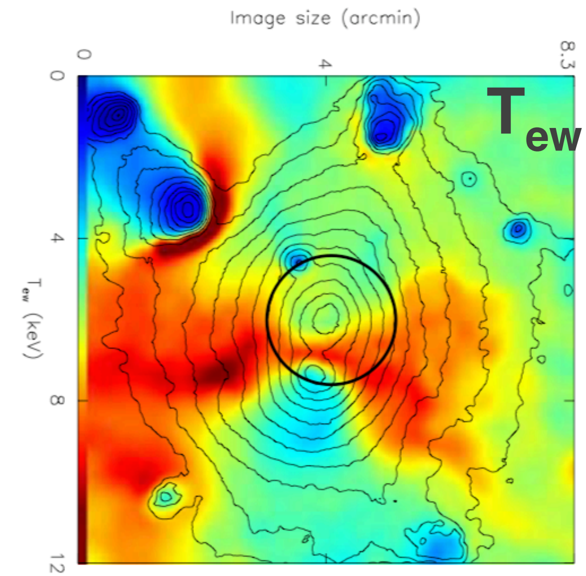

What do we measure in sim

Mass-weighted temperature:

$$T_{\rm mw} \equiv \frac{\int m T \, {\rm d}V}{\int m \, {\rm d}V}$$

Emission-weighted temperature:

$$T_{\rm ew} \equiv \frac{\int \Lambda(T) n^2 T \, {\rm d}V}{\int \Lambda(T) n^2 \, {\rm d}V}$$

Spectroscopic-like temperature:

$$T_{\rm sl} = \frac{\int W T \, {\rm d}V}{\int W \, {\rm d}V} \quad W = \frac{n^2}{T^{3/4}}$$

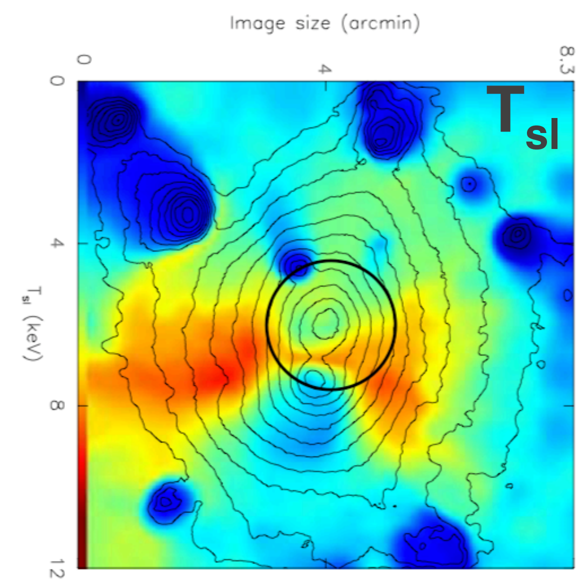

→ Proxy of the temperature from spectral fitting, accounting for thermal complexity of the ICM

X-ray temperature bias

- T_{sl} is a close proxy to the temperature obtained from spectral fitting, *in a Chandra- or XMM-like setup*
- Sizeble difference between T_{ew} and T_{sl}
- T_{sl} lower due to larger weight of cooler regions

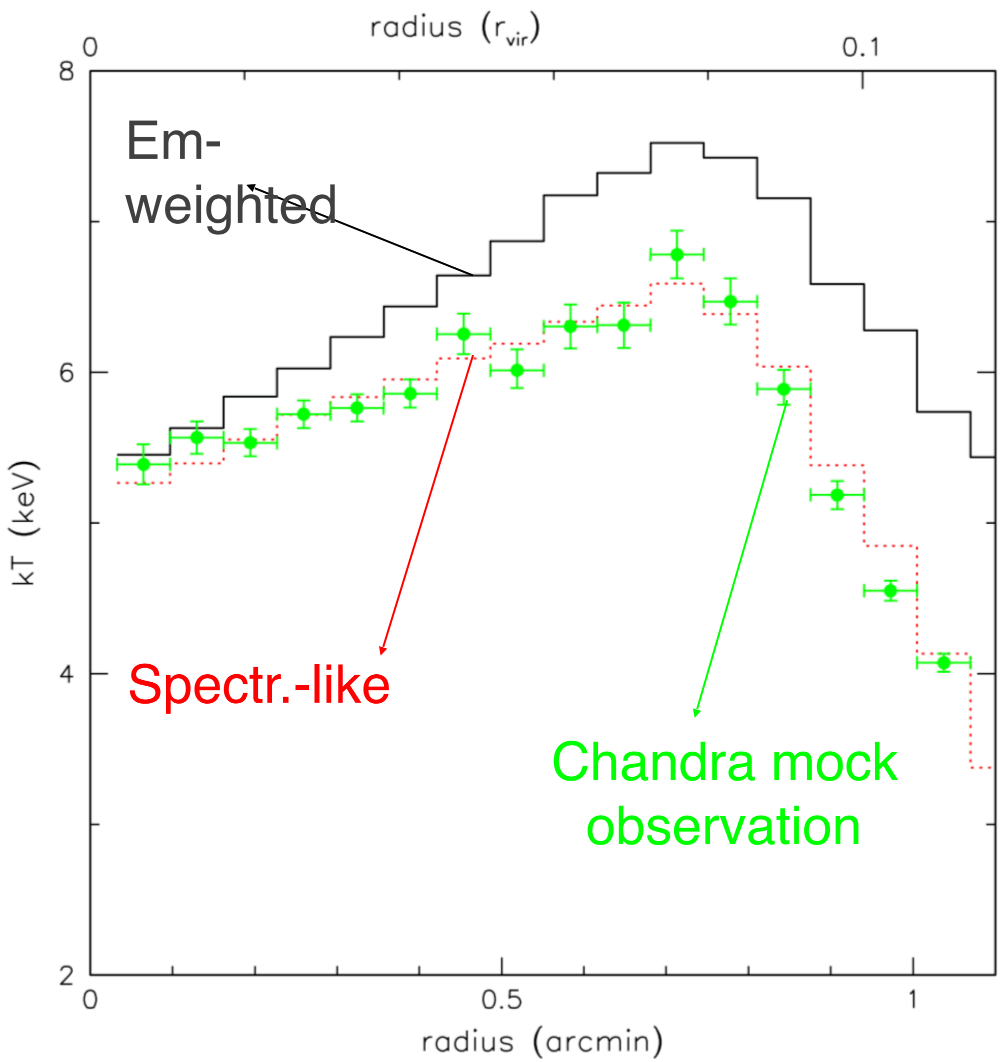

X-ray temperature bias

- T_{sl} is a close proxy to the temperature obtained from spectral fitting, *<u>in a Chandra- or XMM-like setup</u>*
- Sizeble difference between T_{ew} and T_{sl}
- T_{sl} lower due to larger weight of cooler regions

- Small but sizeable mass-bias that adds to the HE bias
- Effect dependent on the thermal complexity of the ICM

→ Not trivial to calibrate with simulations

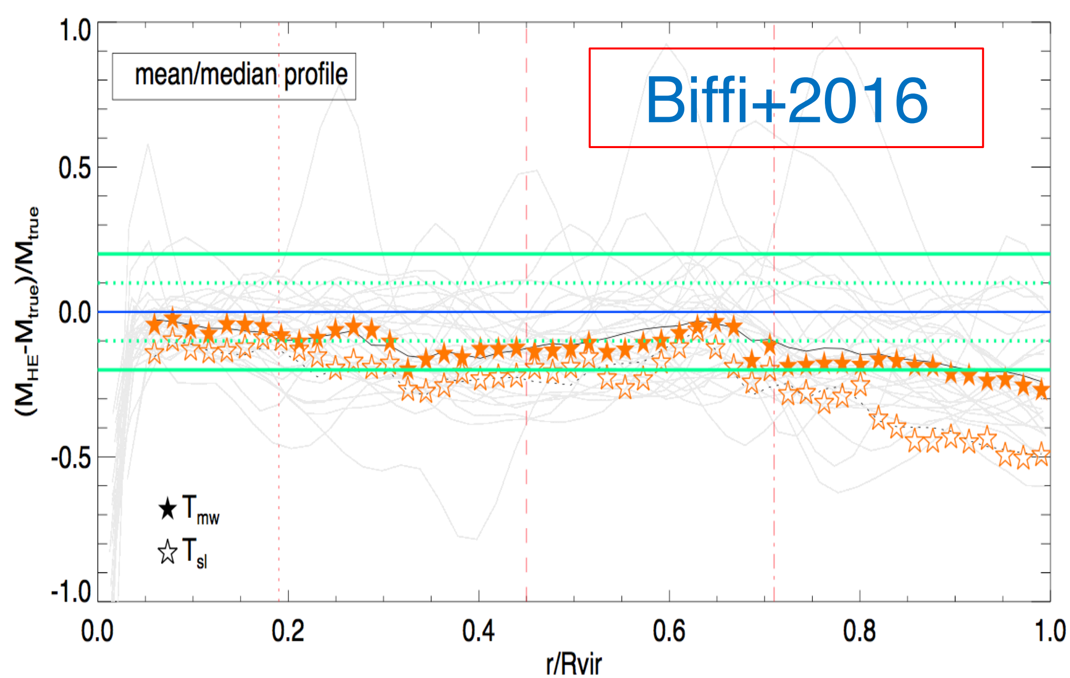

Testing the reliability of WL masses

Idealized mass reconstruction, i.e. no observational effects included

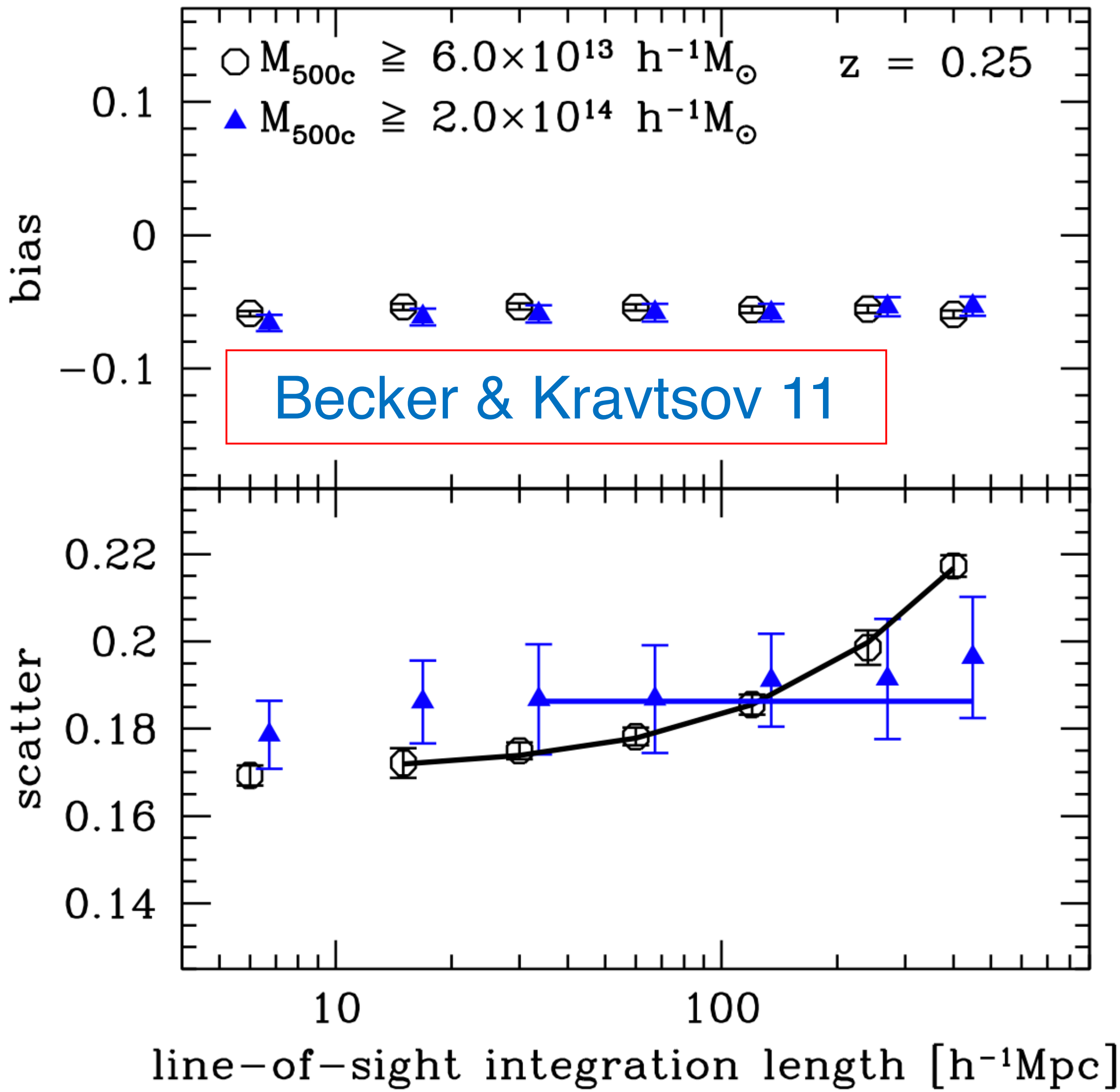

See lectures by A. Heavens

- ➔ Clusters identified in a large (1 Gpc/h) N-body cosmological simulation
- ➔ Spherical NFW fitting to tangential shear profile
- ➔ 5-10% negative bias in recovered masses
- ➔ Significant bias induced by triaxial halo shape, correlated and uncorrelated structures

X-ray and WL masses

HST-WFC3 lensing of a massive simulated cluster at z=0.25

➔ Based on the SkyLens tool (Meneghetti+08)

Meneghetti+08

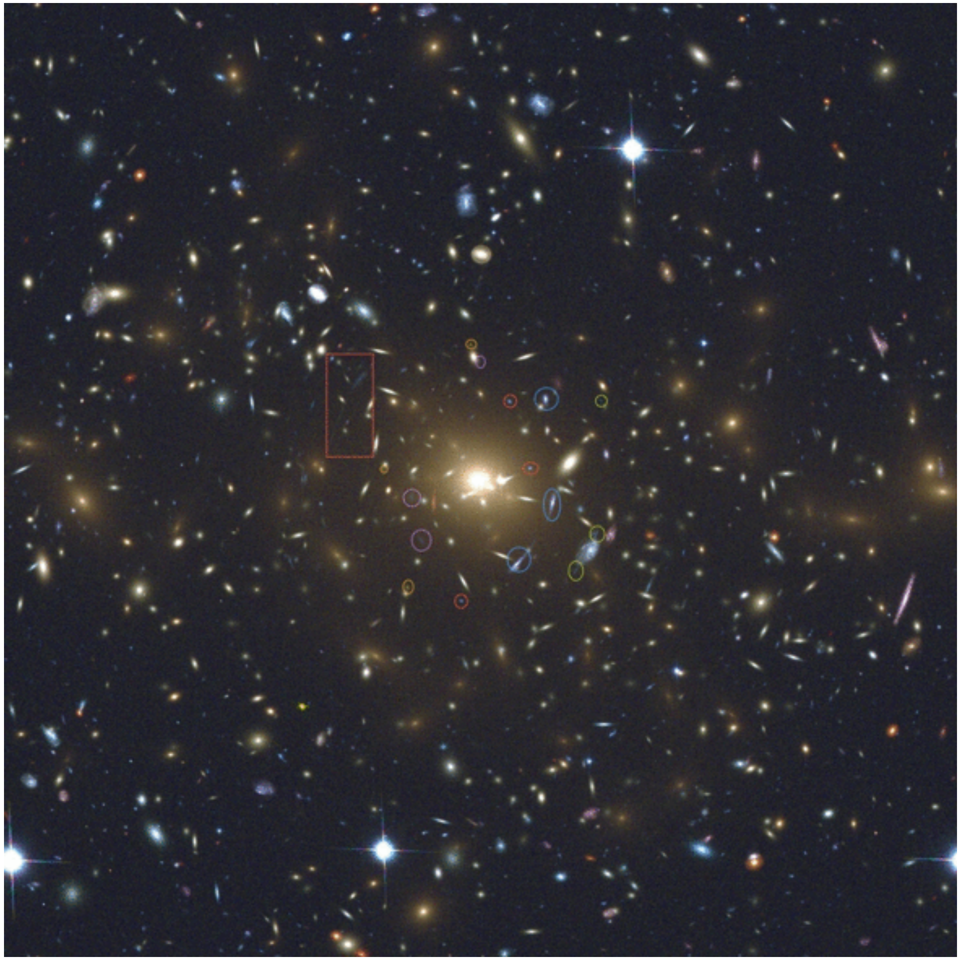

➔ 20 clusters @ z=0.25 with $M_{200} > 5 \times 10^{14}\ M_{\odot}$

➔ 3 projections for each cluster

➔ Generate Subaru SuprimeCam mock lensing observations

➔ Generate Chandra mock event files

➔ Quantitative assessment of (some) observational biases

X-ray and WL masses

HST-WFC3 lensing of a massive simulated cluster at z=0.25
→ Based on the SkyLens tool (Meneghetti+08)

Meneghetti+08

Event files from X-MAS Chandra simulator with 100 ks exp. time
→ [0.7-2] keV X-ray image (16 x 16 $arcmin^2$)

Rasia+12

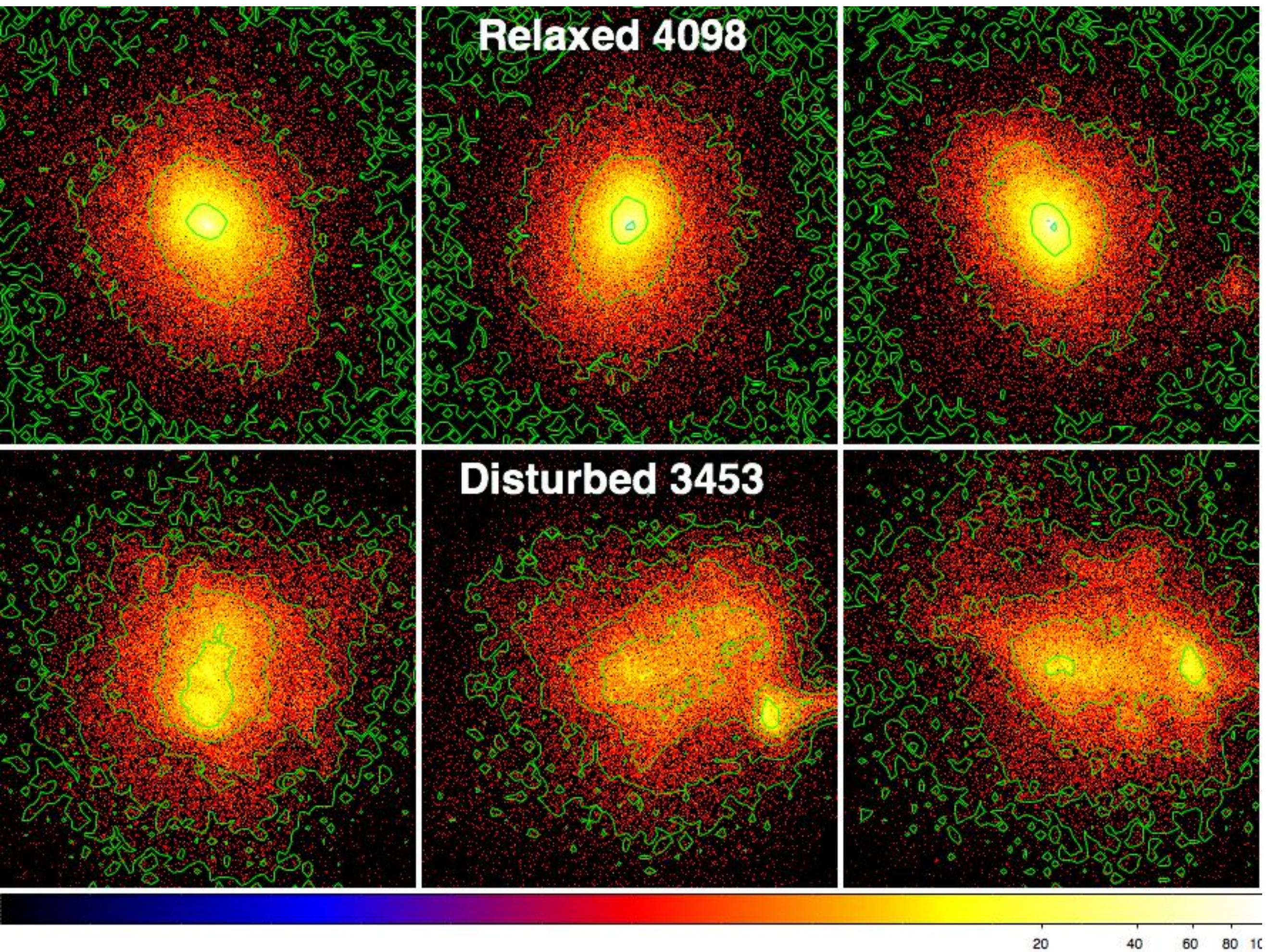

→ 20 clusters @ z=0.25 with $M_{200} > 5 \times 10^{14}\ M_\odot$

→ 3 projections for each cluster

→ Generate Subaru SuprimeCam mock lensing observations

→ Generate Chandra mock event files

→ Quantitative assessment of (some) observational biases

Origin of X-ray mass bias

Black: M_X/M_{true} Red: M_X/M_{true} using T_{mw} Green: M_X/M_{WL}

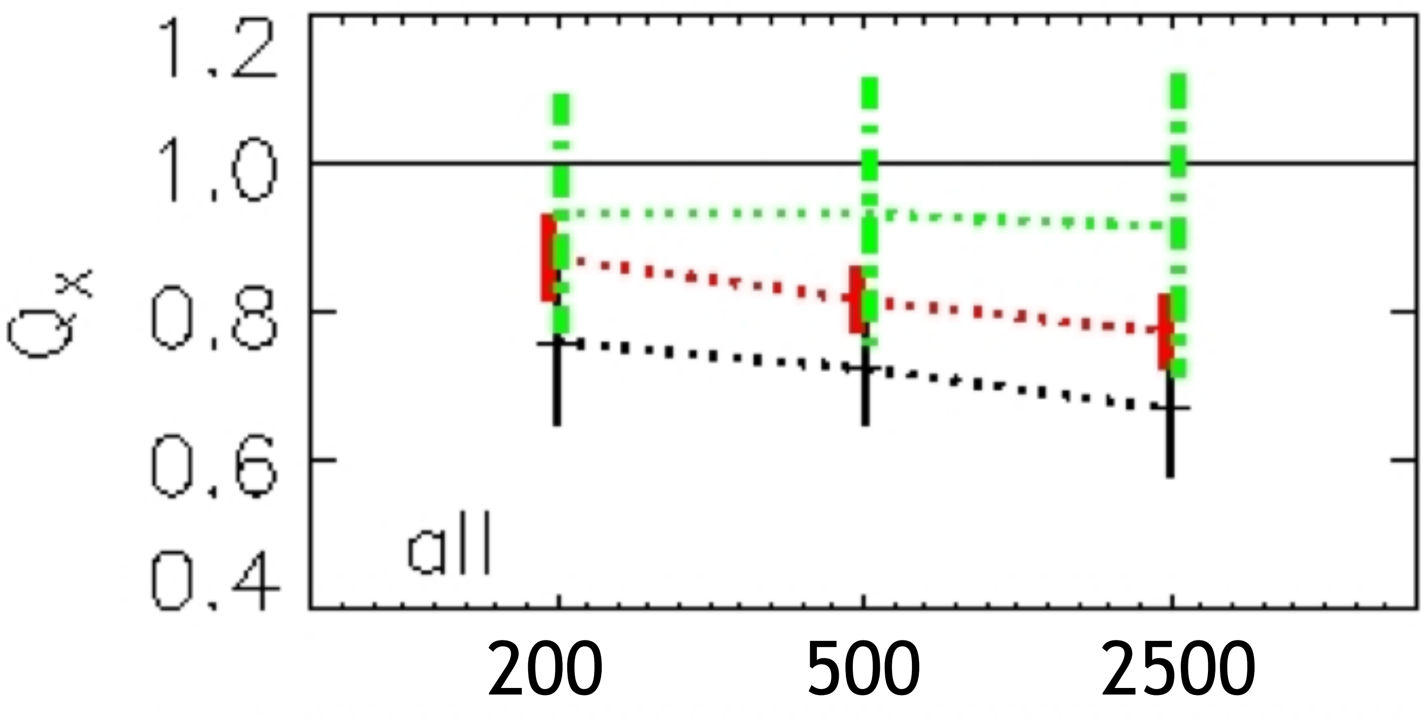

<u>Bias in X-ray masses:</u>

➔ 10-15% from violation of hydrostatic equilibrium

➔ ~15-20% from bias in X-ray temperature estimate (**Q:** simulations reliable?)

<u>Bias in WL masses:</u> ~10% underestimate at R_{500} (also Becker & Kravtsov 11)

The Future

The future

SPT-3G

- 2500 sq.deg.
- ~16,000 receivers (~1000 in SPT-SZ)
- Frequencies: 95, 150, 220 GHz
- $\sim 10^4$ clusters to be detected
- Detect clusters out to z~2 and $M \sim 10^{14}\ M_\odot$

→ NOW TAKING DATA

The future

SPT-3G

- 2500 sq.deg.
- ~16,000 receivers (~1000 in SPT-SZ)
- Frequencies: 95, 150, 220 GHz
- ~10^4 clusters to be detected
- Detect clusters out to z~2 and M~10^{14} $M_\odot$

→ NOW TAKING DATA

eROSITA

- All sky-survey
- Survey speed: 4 times larger than XMM
- PSF: 28” in survey mode
- ~10^5 clusters to be detected
- Secure all clusters > 10^{15} $M_\odot$
- Launch in Sept. 2019

The future

SPT-3G

- 2500 sq.deg.

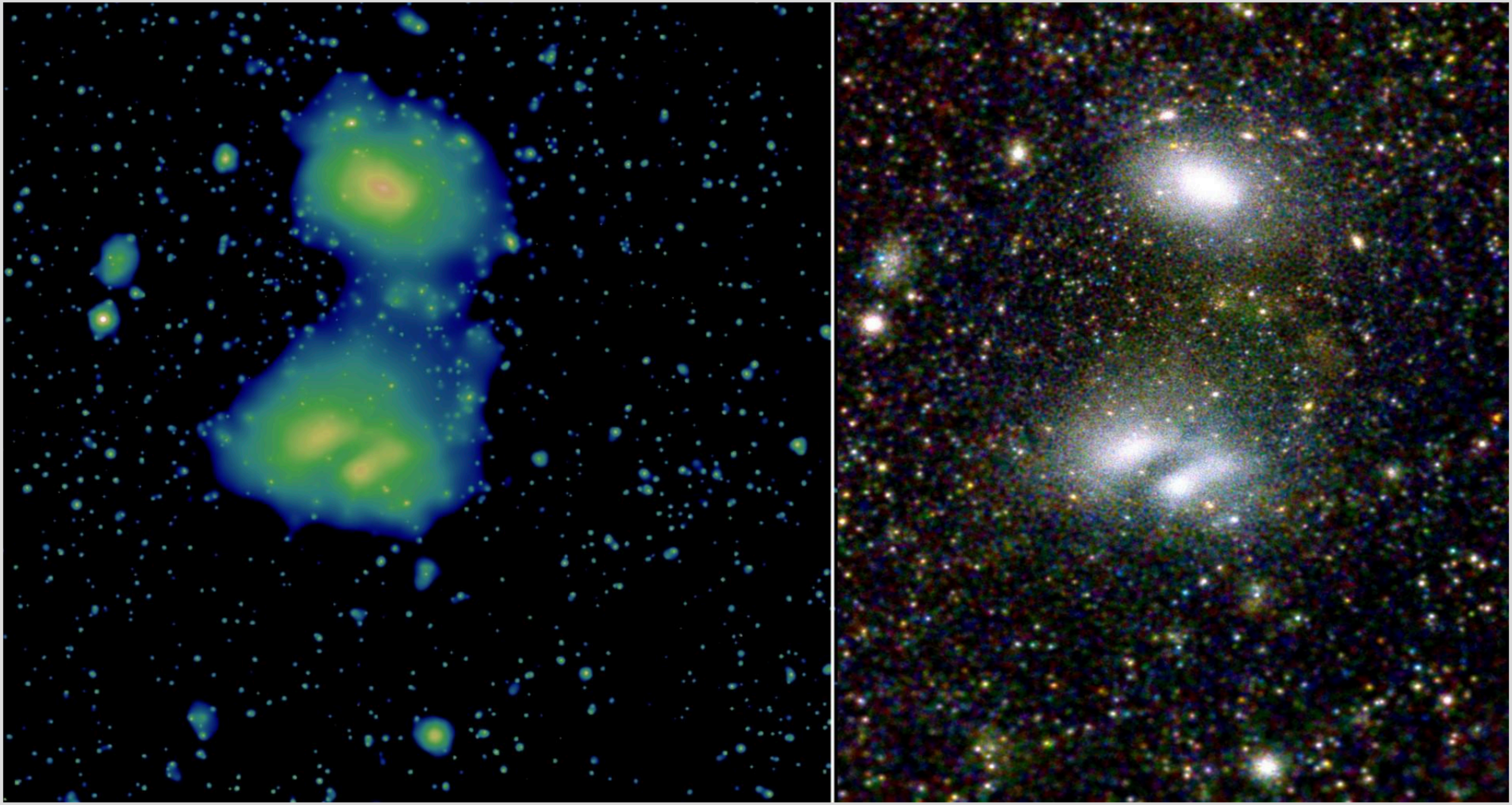

Two interacting galaxy clusters, A3391 and A3395
Image 2/2, **Image:** T. Reiprich (Univ. Bonn), M. Ramos-Ceja (MPE), F. Pacaud (Univ. Bonn), D. Eckert (Univ. Geneva), J. Sanders (MPE), N. Ota (Univ. Bonn), E. Bulbul (MPE), V. Ghirardini (MPE), MPE/IKI

- Launch in Sept. 2019

The future

Euclid

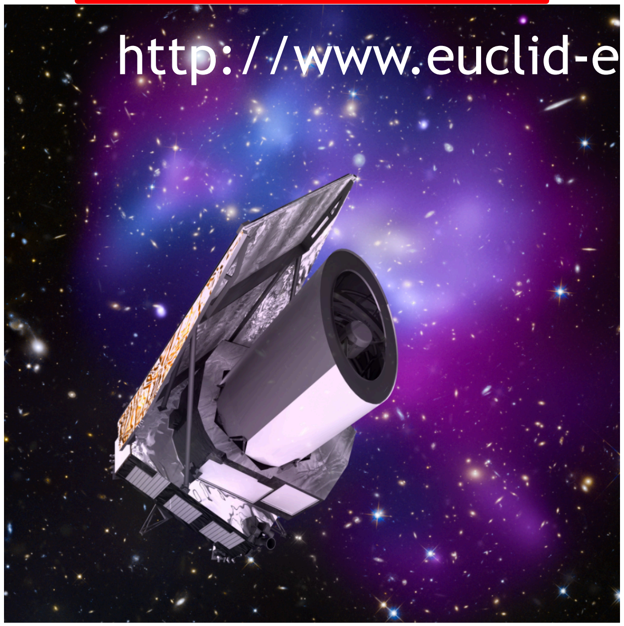

An artist view of the Euclid Satellite – © ESA

- 1.2m mirror
- Optical imaging
- NIR (YJH) photometry & NIR grism
- 15,000 sq.deg. to be covered
- Launch in 2021
- Cosmology
    - Cosmic shear
    - BAO & RSD
    - Galaxy clusters

The future

Euclid

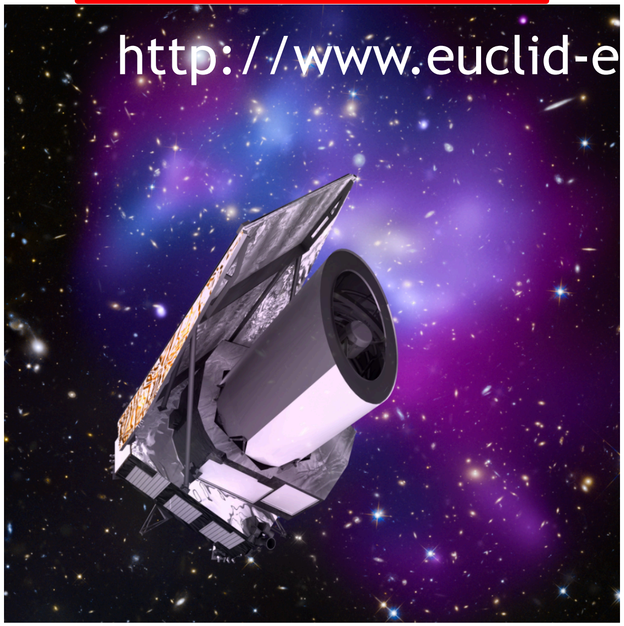

An artist view of the Euclid Satellite – © ESA

- 1.2m mirror
- Optical imaging
- NIR (YJH) photometry & NIR grism
- 15,000 sq.deg. to be covered
- Launch in 2021
- Cosmology
  - Cosmic shear
  - BAO & RSD
  - Galaxy clusters

LSST

- 8.4m mirror
- *ugrizy* photometry
- ~18,000 sq.deg. to be covered
- Operations to start in 2022
- Highly complementary to Euclid
- Similar/complementary science cases and cosmological probes

The Euclid Cluster Survey

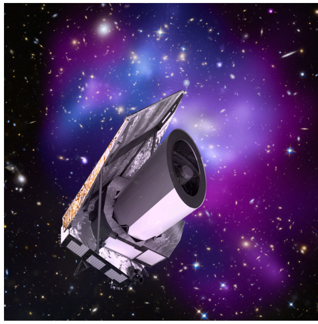

An artist view of the Euclid Satellite – © ESA

Sartoris+2016

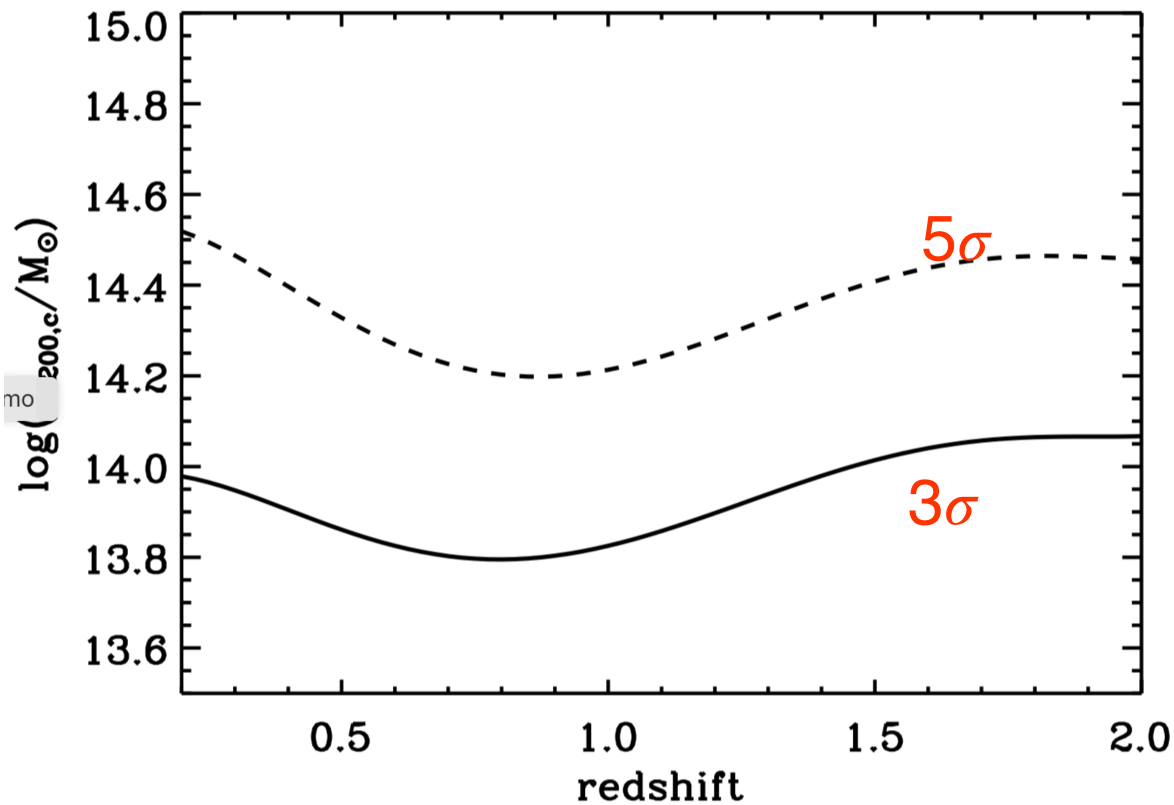

- Selection function for photometric cluster identification in the Euclid wide survey (H_{AB}<24)

The Euclid Cluster Survey

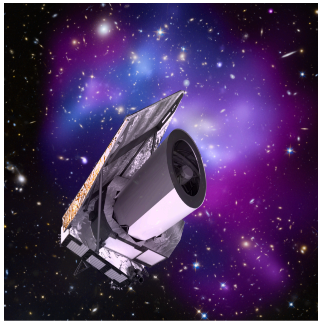

An artist view of the Euclid Satellite – © ESA

Sartoris+2016

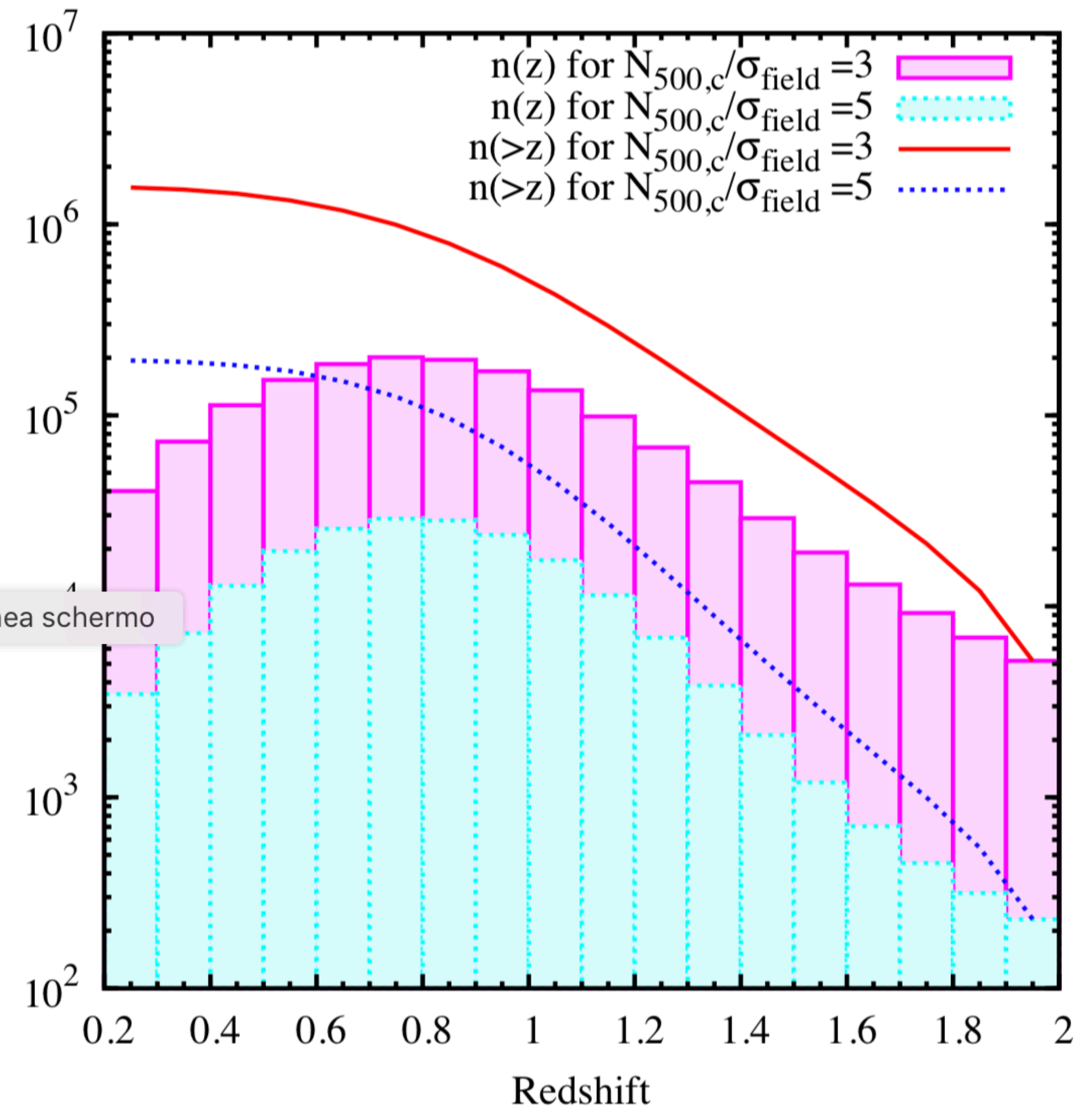

- Selection function for photometric cluster identification in the Euclid wide survey (H_{AB}<24)
- ~10^6 clusters to be found
- ~few x 10^5 at z>1

➔ Statistics not an issue!

Q: take them all, including systematics, or select a "golden" sample with many fewer clusters?

WL masses with Euclid

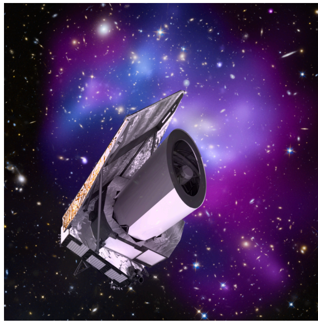

An artist view of the Euclid Satellite – © ESA

Minimum WL mass estimated with a certain accuracy (Giocoli+18)

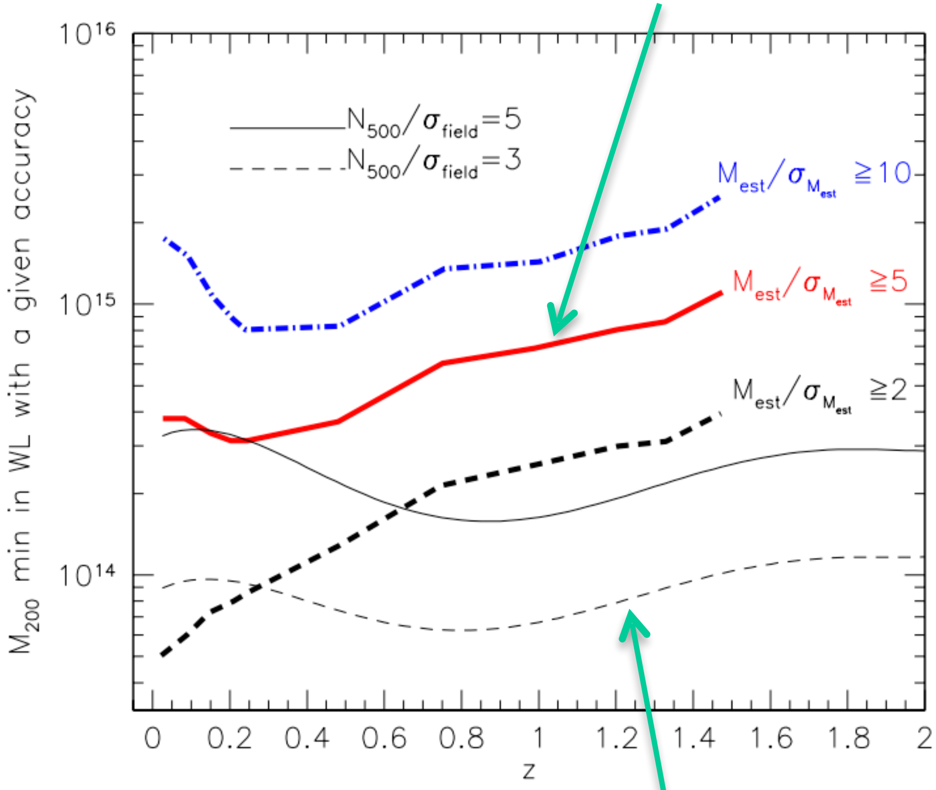

Photometric selection function
Sartoris+2016

Expected no. of clusters with WL mass at a given accuracy

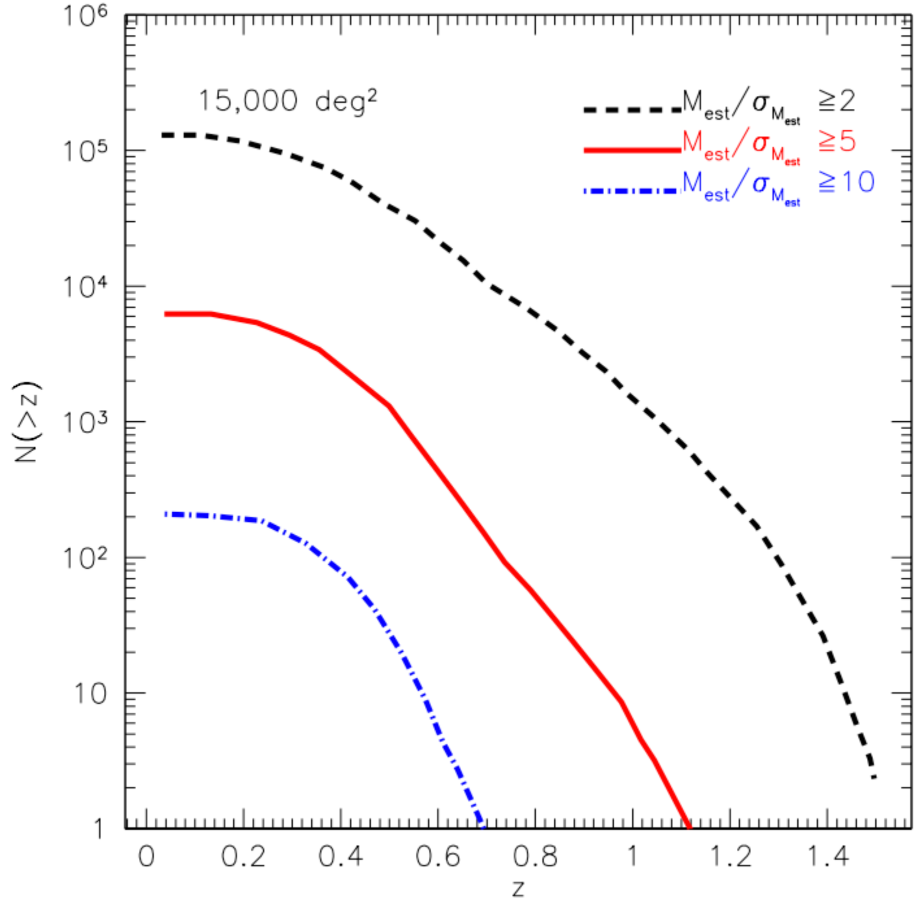

Cosmology with Euclid Clusters

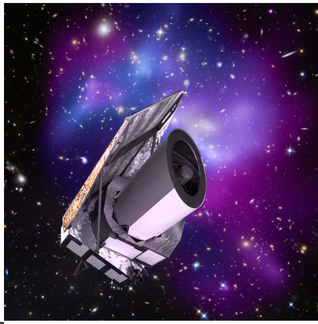

An artist view of the Euclid Satellite – © ESA

Sartoris+15

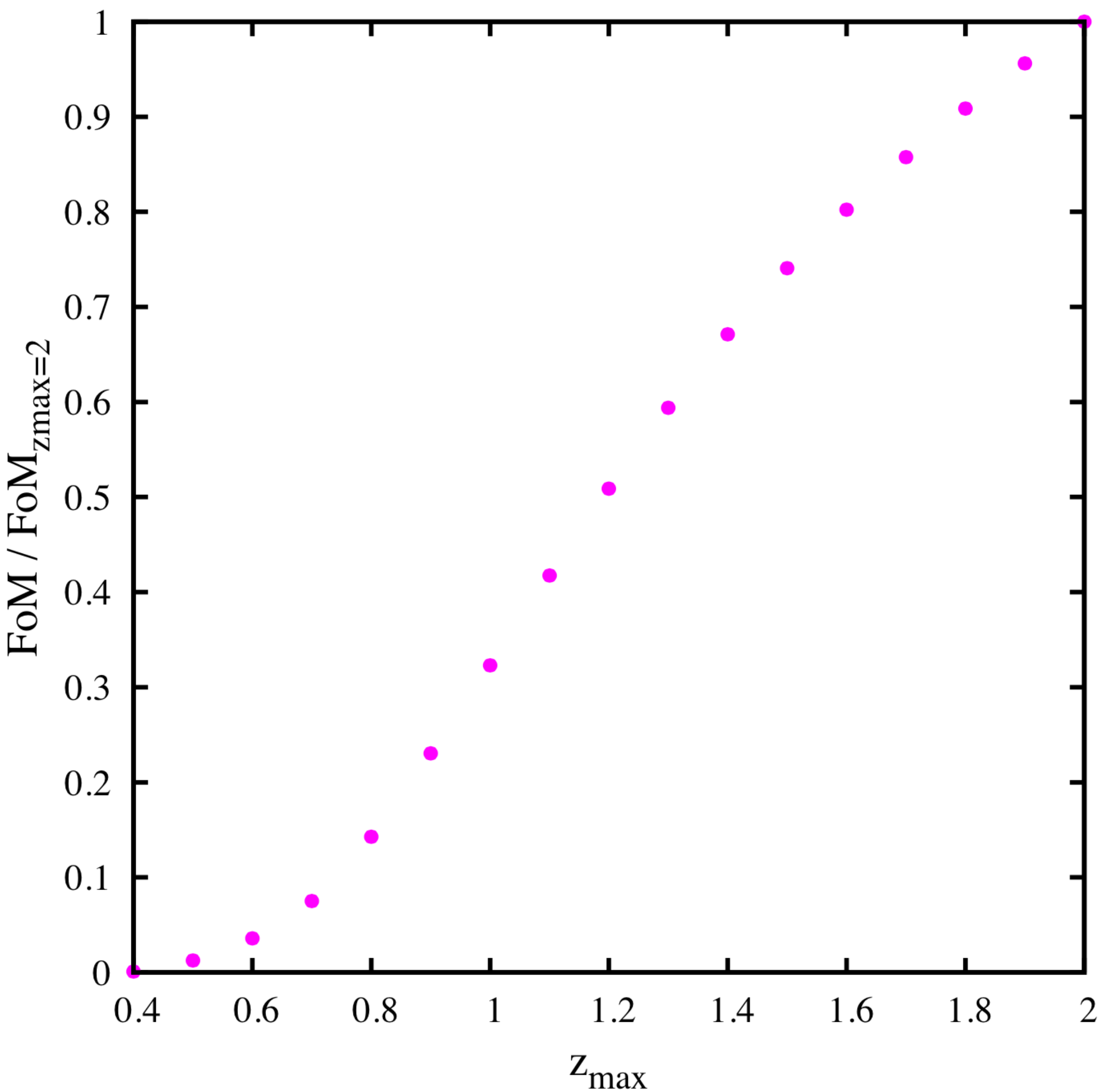

DE equation of state

$$w(a) = w_0 + w_a(1-a)$$

$$\mathrm{FoM} = \frac{1}{\sqrt{\det\left[Cov\left(p_i, p_j\right)\right]}}$$

Cosmology with Euclid Clusters

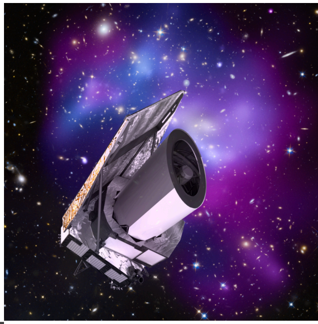

Sartoris+15

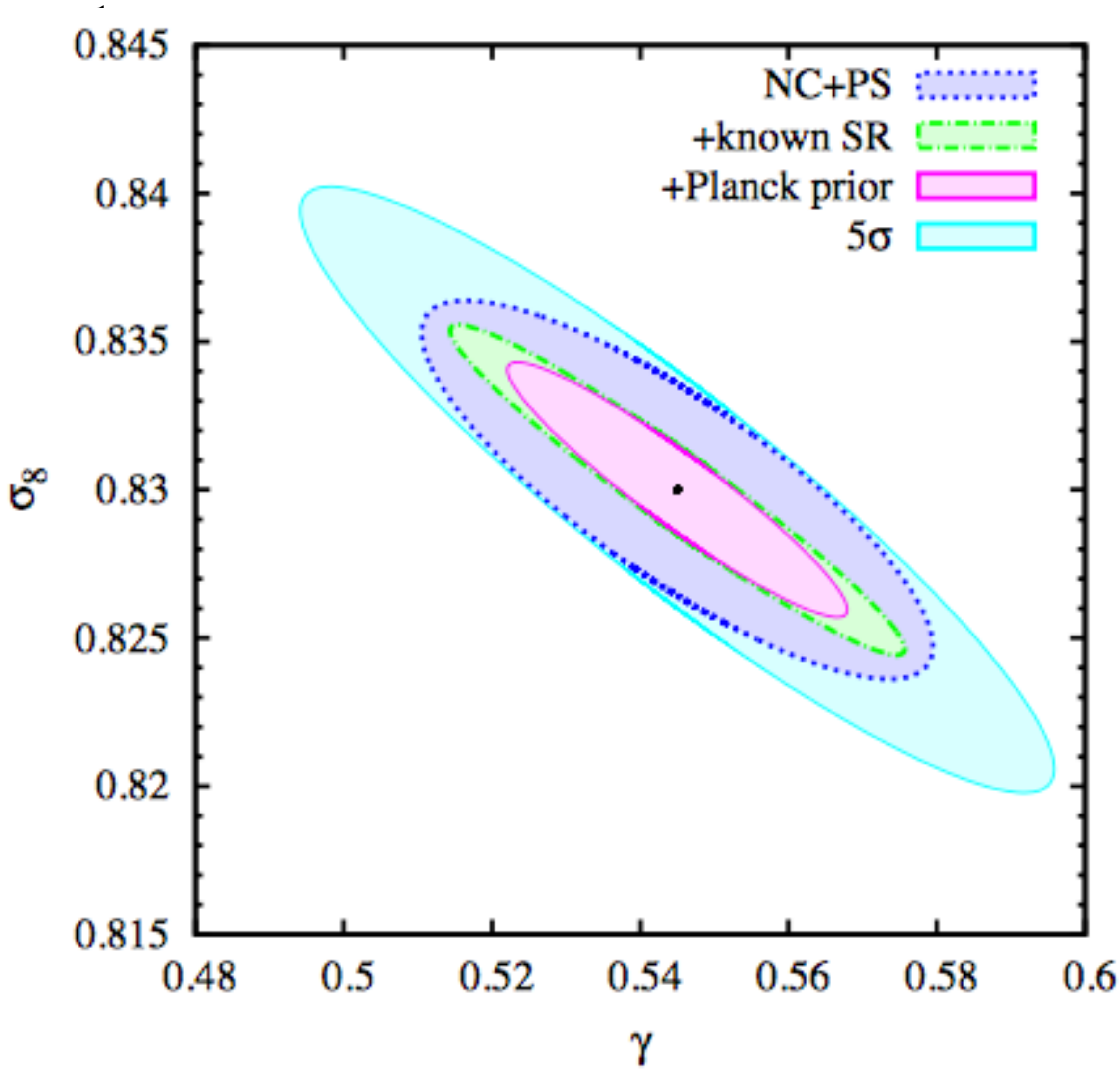

DE equation of state

$$w(a) = w_0 + w_a(1-a)$$

$$\mathrm{FoM} = \frac{1}{\sqrt{\det\left[Cov\left(p_i, p_j\right)\right]}}$$

The power of pushing to z>1:

➔ About 70% of FoM from clusters at z>1

$$\frac{d\ln\delta}{d\ln a} = \Omega_m(a)^\gamma$$

➔ σ_γ=0.02: >1 order of magnitude improvement wrt current constraints

Take home messages

- Huge potential of galaxy clusters for cosmology!
- Cosmological simulations as useful guidelines to
  → understand and calibrate biases in mass measurements
  → assess precision and robustness of mass proxies
- Mind: observational data will tell the final word on this!
- All this under control at the level required by current surveys
- Next generation surveys require a quantum leap in the control of all these systematics!

Take home messages

- Huge potential of galaxy clusters for cosmology!
- Cosmological simulations as useful guidelines to
  - ➔ understand and calibrate biases in mass measurements
  - ➔ assess precision and robustness of mass proxies
- <u>Mind</u>: observational data will tell the final word on this!
- All this under control at the level required by current surveys
- Next generation surveys require a quantum leap in the control of all these systematics!

➔ Cluster cosmology is much more than counting clusters!

➔ Lots of astrophysics to understand in the process….